

Functional antibody and T-cell immunity following SARS-CoV-2 infection, including by variants of concern, in patients with cancer: the CAPTURE study

Annika Fendler
Lewis Au
Scott Shepherd
Fiona Byrne
Maddalena Cerrone
Laura Boos
Karolina Rzeniewicz
William Gordon
Ben Shum
Camille Gerard
Barry Ward
Wenyi Xie
Andreas Schmitt
Nalinie Joharatnam-Hogan
Georgina Cornish
Martin Pule
Leila Mekkaoui
Kevin Ng
Eleanor Carlyle
Kim Edmonds
Lyra Del Rosario
Sarah Sarker
Karla Lingard
Mary Mangwende
Lucy Holt
Hamid Ahmod
Richard Stone
Camila Gomes
Helen Flynn
Ana Agua-Doce
Philip Hobson
Simon Caidan

Michael Howell
Mary Wu
Robert Goldstone
Margaret Crawford
Laura Cubitt
Harshil Patel
Mike Gavrielides
Emma Nye
Ambrosius Snijders
James MacRae
Jerome Nicod
Firza Gronthoud
Robyn Shea
Christina Messiou
David Cunningham
Ian Chau
Naureen Starling
Nicholas Turner
Liam Welsh
Nicholas van As
Robin Jones
Joanne Droney
Susana Banerjee
Kate Tatham
Shaman Jhanji
Mary O'Brien
Oliva Curtis
Kevin Harrington
Shreerang Bhide
Jessica Bazin
Anna Robinson
Clemency Stephenson
Tim Slattery
Yasir Khan
Zayd Tippu
Isla Leslie
Spyridon Gennatas
Alicia Okines
Alison Reid
Kate Young
Andrew Furness
Lisa Pickering

Sonia Gandhi
Steve Gamblin
Charles Swanton
Emma Nicholson
Sacheen Kumar
Nadia Yousaf
Katalin Wilkinson
Anthony Swerdlow
Ruth Harvey
George Kassiotis
James Larkin
Robert Wilkinson
Samra Turajlic (✉ samra.turajlic@crick.ac.uk)

Research Article

Keywords: SARS-CoV-2, COVID-19, Cancer, Adaptive Immunity, Antibody Response, Neutralising Antibodies, T-cell Response, Prospective Study, Vaccine

Posted Date: September 20th, 2021

DOI: <https://doi.org/10.21203/rs.3.rs-916427/v1>

License:  This work is licensed under a Creative Commons Attribution 4.0 International License.

[Read Full License](#)

1 **Functional antibody and T-cell immunity following SARS-CoV-2 infection,**
2 **including by variants of concern, in patients with cancer: the CAPTURE study**

3
4 Annika Fendler^{1,43}, Lewis Au^{1,2,43}, Scott T.C. Shepherd^{1,2,43}, Fiona Byrne¹, Maddalena Cerrone^{3,4}, Laura
5 Amanda Boos², Karolina Rzeniewicz¹, William Gordon¹, Ben Shum^{1,2}, Camille L. Gerard¹, Barry Ward¹,
6 Wenyi Xie¹, Andreas M. Schmitt², Nalinie Joharatnam-Hogan², Georgina H. Cornish⁵, Martin Pule^{6,7},
7 Leila Mekkaoui⁷, Kevin W. Ng⁵, Eleanor Carlyle², Kim Edmonds², Lyra Del Rosario², Sarah Sarker²,
8 Karla Lingard², Mary Mangwende², Lucy Holt², Hamid Ahmod², Richard Stone⁷, Camila Gomes⁷, Helen
9 R. Flynn⁹, Ana Agua-Doce¹⁰, Philip Hobson¹⁰, Simon Caidan¹¹, Michael Howell¹², Mary Wu¹², Robert
10 Goldstone¹³, Margaret Crawford¹³, Laura Cubitt¹³, Harshil Patel¹⁴, Mike Gavrielides¹⁵, Emma Nye⁸,
11 Ambrosius P Snijders⁹, James I MacRae¹⁶, Jerome Nicod¹³, Firza Gronthoud¹⁷, Robyn L. Shea^{17,18},
12 Christina Messiou¹⁹, David Cunningham²⁰, Ian Chau²⁰, Naureen Starling²⁰, Nicholas Turner²¹, Liam
13 Welsh²², Nicholas van As²³, Robin L. Jones²⁴, Joanne Droney²⁵, Susana Banerjee²⁶, Kate C. Tatham²⁷,
14 Shaman Jhanji²⁷, Mary O'Brien²⁸, Olivia Curtis²⁸, Kevin Harrington^{29,30}, Shreerang Bhide²⁹, Jessica
15 Bazin³¹, Anna Robinson³¹, Clemency Stephenson³¹, Tim Slattery², Yasir Khan², Zayd Tippu², Isla
16 Leslie², Spyridon Gennatas^{32,33}, Alicia Okines^{21,32}, Alison Reid³⁴, Kate Young², Andrew J.S. Furness²,
17 Lisa Pickering², Sonia Gandhi^{35,36}, Steve Gamblin³⁷, Charles Swanton^{38,39} on behalf of the Crick
18 COVID19 consortium, Emma Nicholson³¹, Sacheen Kumar²⁰, Nadia Yousaf^{28,32}, Katalin A. Wilkinson^{3,42},
19 Anthony Swerdlow⁴⁰, Ruth Harvey⁴¹, George Kassiotis⁵, James Larkin², Robert J. Wilkinson^{3,4,42}, Samra
20 Turajlic^{1,2,*} on behalf of the CAPTURE consortium

21
22 ¹Cancer Dynamics Laboratory, The Francis Crick Institute, London, NW1 1AT, UK

23 ²Skin and Renal Units, The Royal Marsden NHS Foundation Trust, London, SW3 6JJ, UK

24 ³Tuberculosis Laboratory, The Francis Crick Institute, London, NW1 1AT, UK

25 ⁴Department of Infectious Disease, Imperial College London, W12 0NN, UK

26 ⁵Retroviral Immunology Laboratory, The Francis Crick Institute, London, NW1 1AT, UK

27 ⁶Research Department of Haematology at University College London Cancer Institute, WC1E 6DD,
28 London, UK

29 ⁷Autolus Limited, The MediaWorks, 191 Wood Lane, London, W12 7F

30 ⁸Experimental Histopathology Laboratory, The Francis Crick Institute, London, NW1 1AT, UK

31 ⁹Mass Spectrometry Proteomics Science Technology Platform, The Francis Crick Institute, London,
32 NW1 1AT, UK

33 ¹⁰Flow Cytometry Scientific Technology Platform, The Francis Crick Institute, London, NW1 1AT, UK

34 ¹¹Safety, Health & Sustainability, The Francis Crick Institute, London, NW1 1AT, UK
35 ¹²High Throughput Screening Laboratory, The Francis Crick Institute, London, NW1 1AT, UK
36 ¹³Advanced Sequencing Facility, The Francis Crick Institute, London, NW1 1AT, UK
37 ¹⁴Department of Bioinformatics and Biostatistics, The Francis Crick Institute, London, UK.
38 ¹⁵Scientific Computing Scientific Technology Platform, The Francis Crick Institute, London, NW1 1AT,
39 UK
40 ¹⁶Metabolomics Scientific Technology Platform, The Francis Crick Institute, London, NW1 1AT, UK
41 ¹⁷Department of Pathology, The Royal Marsden NHS Foundation Trust, London, NW1 1AT, UK
42 ¹⁸Translational Cancer Biochemistry Laboratory, The Institute of Cancer Research, London, SW7 3RP,
43 UK
44 ¹⁹Department of Radiology, The Royal Marsden NHS Foundation Trust, London, SW3 6JJ, UK
45 ²⁰Gastrointestinal Unit, The Royal Marsden NHS Foundation Trust, London and Surrey SM2 5PT
46 ²¹Breast Unit, The Royal Marsden NHS Foundation Trust, London, SW3 6JJ, UK
47 ²²Neuro-oncology Unit, The Royal Marsden NHS Foundation Trust, London, SW3 6JJ, UK
48 ²³Clinical Oncology Unit, The Royal Marsden NHS Foundation Trust, London, SW3 6JJ, UK
49 ²⁴Sarcoma Unit, The Royal Marsden NHS Foundation Trust and Institute of Cancer Research, London,
50 SW3 6JJ, UK
51 ²⁵Palliative Medicine, The Royal Marsden NHS Foundation Trust, London, SW3 6JJ, UK
52 ²⁶Gynaecology Unit, The Royal Marsden NHS Foundation Trust, London, SW3 6JJ, UK
53 ²⁷Anaesthetics, Perioperative Medicine and Pain Department, The Royal Marsden NHS Foundation
54 Trust, London, SW3 6JJ, UK
55 ²⁸Lung Unit, The Royal Marsden NHS Foundation Trust, London, SW3 6JJ, UK
56 ²⁹Head and Neck, The Royal Marsden NHS Foundation Trust, London, SW3 6JJ, UK
57 ³⁰Targeted Therapy Team, The Institute of Cancer Research, London, SW7 3RP, UK
58 ³¹Haemato-oncology Unit, The Royal Marsden NHS Foundation Trust, London, SW3 6JJ, UK
59 ³²Acute Oncology Service, The Royal Marsden NHS Foundation Trust, London, SW3 6JJ, UK
60 ³³Department of Medical Oncology, 14th Floor, Great Maze Pond Road, Tower Wing, Guy's Hospital,
61 London SE1 9RY, UK
62 ³⁴Uro-oncology unit, The Royal Marsden NHS Foundation Trust, Surrey, SM2 5PT
63 ³⁵Neurodegeneration Biology Laboratory, The Francis Crick Institute, London, NW1 1AT, UK
64 ³⁶UCL Queen Square Institute of Neurology, Queen Square, London WC1N 3BG
65 ³⁷Structural Biology of Disease Processes Laboratory, The Francis Crick Institute, London, NW1 1AT,
66 UK

67 ³⁸Cancer Evolution and Genome Instability Laboratory, The Francis Crick Institute, London, NW1 1AT,

68 UK

69 ³⁹University College London Cancer Institute, London WC1E 6DD, UK

70 ⁴⁰Division of Genetics and Epidemiology and Division of Breast Cancer Research, The Institute of

71 Cancer Research, London, SW7 3RP, UK

72 ⁴¹Worldwide Influenza Centre, The Francis Crick Institute, London, NW1 1AT, UK

73 ⁴²Wellcome Center for Infectious Disease Research in Africa, University Cape Town, Observatory

74 7925, Republic of South Africa

75 ⁴³Equal contribution

76

77

78

79 **Keywords:** SARS-CoV-2, COVID-19, Cancer, Adaptive Immunity, Antibody Response, Neutralising

80 Antibodies, T-cell Response, Prospective Study, Vaccine

81

82

83 ***Corresponding author:** Dr Samra Turajlic

84 Telephone: +44 020 37961111

85 E-mail: samra.turajlic@crick.ac.uk

86

87

88

89

90 **Abstract**

91 Patients with cancer have higher COVID-19 morbidity and mortality. Here we present the
92 prospective CAPTURE study (NCT03226886) integrating longitudinal immune profiling with clinical
93 annotation. Of 357 patients with cancer, 118 were SARS-CoV-2-positive, 94 were symptomatic and 2
94 patients died of COVID-19. In this cohort, 83% patients had S1-reactive antibodies, 82% had
95 neutralizing antibodies against WT, whereas neutralizing antibody titers (NAbT) against the Alpha,
96 Beta, and Delta variants were substantially reduced. Whereas S1-reactive antibody levels decreased
97 in 13% of patients, NAbT remained stable up to 329 days. Patients also had detectable SARS-CoV-2-
98 specific T cells and CD4+ responses correlating with S1-reactive antibody levels, although patients
99 with hematological malignancies had impaired immune responses that were disease and treatment-
100 specific, but presented compensatory cellular responses, further supported by clinical. Overall, these
101 findings advance the understanding of the nature and duration of immune response to SARS-CoV-2
102 in patients with cancer.

103
104
105
106
107
108
109
110
111
112
113
114
115
116
117
118
119
120
121

122 **Introduction**

123 Patients with cancer have an increased risk of severe outcomes from coronavirus disease 2019
124 (COVID-19),^{1,2} with risk factors including general (e.g. increased age, male sex, obesity, co-
125 morbidities) as well as cancer-specific features (e.g. haematological and thoracic malignancies,
126 active cancer, poor performance status).³⁻⁸ The precise effects of anti-cancer treatments on the
127 course and outcome of SARS-CoV-2 infection are yet to be fully understood, with different reports
128 yielding conflicting results.^{5,7,9,10} Understanding of the immune response to SARS-CoV-2 in this
129 heterogeneous population, spanning multiple malignancy types and numerous treatment regimens,
130 is crucial for optimal clinical management of those patients during the ongoing pandemic.

131 Calibration of current and future risk-mitigation measures, including risk of re-infection and
132 vaccine effectiveness, requires an understanding of the impact of cancer and cancer treatments on
133 the nature, extent and duration of immunity to SARS-CoV-2. Previous studies established an acute
134 immune response to SARS-CoV-2 in cancer patients, with 1) solid tumour patients showing high
135 seroconversion rates, and 2) haematological cancer patients showing impaired humoral immunity,
136 especially under anti-CD20 treatments, but with improved survival in those with higher CD8+ T-cell
137 counts.¹¹⁻¹³ However, features of the immune response (including SARS-CoV-2-specific T-cells and
138 neutralising antibodies), and their correlation with clinical characteristics in large non-hospitalized
139 cancer cohorts, and cross-protection against emerging variants of concern (VOC) remain unknown.

140 CAPTURE (COVID-19 antiviral response in a pan-tumour immune monitoring study) is a
141 prospective, longitudinal cohort study initiated in response to the global SARS-CoV-2 pandemic and
142 its impact on cancer patients.¹⁴ The study evaluates the impact of cancer and cancer therapies on
143 the immune response to SARS-CoV-2 infection and COVID-19 vaccinations. Here, we report findings
144 from the SARS-CoV-2 infection cohort of the study.

145

146 **Results**

147 **Patient demographics and baseline characteristics**

148 Between May 4, 2020 and March 31st 2021 (database lock), 357 unvaccinated cancer patients were
149 evaluable and followed-up for a median of 154 days (IQR: 63-273). Median age was 59 years, 54%
150 were male, 89% had solid malignancy, and the majority (64%) had advanced disease (**Table 1**).
151 Overall, 118 patients (33%; 97 with solid cancers and 21 with haematological malignancies), were
152 classified as SARS-CoV-2-positive according to our case definition (positive SARS-CoV-2 RT-PCR
153 and/or ELISA for S1-reactive antibodies, at/or prior to study enrolment), and were included in the
154 analysis (**Figure 1a,b, see Methods**). The most common comorbidities were hypertension (27%),
155 obesity (21%) and diabetes mellitus (11%); no significant baseline differences were observed
156 between patients with solid and haematological malignancies (**Table 2, Supplementary Table 1**).
157 Overall, 88% patients received SACT (51% chemotherapy; 21% targeted therapy; 12% immune
158 checkpoint inhibitors [CPI]; 5% anti-CD20), 10% had radiotherapy and 13% underwent surgery in the
159 12 weeks prior to infection. Response to the most recent anti-cancer intervention is shown in **Table**
160 **2**.

161

162 **Viral shedding and lineage**

163 SARS-CoV-2 infection was confirmed by SARS-CoV-2 RT-PCR in 95/118 patients (81%). Repeat testing
164 was not mandated by study protocol but 40% (47/118) had longitudinal swabs in the course of
165 routine care. Within this group, the estimated median duration of viral shedding (see **Methods**) was
166 12 days (range: 6-80) (**Figure 1c, Table 3**), with evidence of prolonged shedding in patients with
167 haematological malignancies (median 21 vs 12 days in patients with solid cancers) (**Extended Data**
168 **Figure 1a**). Duration of viral shedding was not correlated with COVID-19 severity ($r = 0.04$, $p = 0.7$).
169 We performed viral sequencing in 52 RT-PCR-positive samples with Ct > 32, of which 44/52 passed
170 sequencing quality control. The Alpha VOC accounted for the majority of infections in our cohort
171 between December 2020 and March 2021, consistent with community prevalence in the UK
172 (**Extended Data Figure 1b**).

173

174 **Clinical correlates of COVID-19 severity in cancer patients**

175 Overall, 94 patients (80%) were symptomatic, of whom 52 (44%) had mild, 36 (31%) moderate, and 6
176 (5%) severe illness (as per the WHO severity scale,¹⁵ **Table 3**); 24 patients (20%) were asymptomatic
177 (WHO score 1). Among all patients (n=118), fever (47%), cough (42%), gastro-intestinal symptoms
178 (12%), and dyspnoea (31%) were the most common presenting symptoms (**Figure 1d**), with a
179 median of 2 symptoms reported (range: 0-7). In patients with a clear date of symptom resolution

180 (n=77), duration of symptoms was 18 days (IQR: 11-30). Three patients met the criteria of long
181 COVID (symptomatic > 90 days since presentation of disease (POD)), all following severe COVID-19
182 requiring ITU care.

183 Thirty-three patients (28%) were hospitalised due to COVID-19, with a median duration of
184 in-patient stay of nine days (range: 1-120); 27 (23%) required supplemental oxygen, seven (6%) were
185 admitted to an intensive care unit (ICU), with one (1%) requiring mechanical ventilation and
186 inotropic support (**Table 3**). Thirteen patients (11%) were treated with corticosteroids (>10 mg
187 prednisolone equivalent), and three patients (3%) received tocilizumab. Nine patients (8%) had a
188 thrombo-embolic complication. At database lock, eleven SARS-CoV-2-positive patients (9%) died of
189 progressive cancer, and two patients (2%) died due to recognised complications of COVID-19 (**Table**
190 **3**).

191 The risk of moderate and severe COVID-19 was associated with haematological
192 malignancies, while risk of severe COVID-19 in solid malignancies was associated with progressive
193 disease under SACT (**Supplementary Table 2**), in line with previous reports^{7,8,12}. We found no
194 association between COVID-19 severity, cancer stage, performance status, sex, age, obesity, smoking
195 status or comorbidities across the whole cohort, though positive association of these factors were
196 noted in registries largely reporting on cancer patients hospitalised with COVID-19^{4,7,8,16,17}.

197

198 **Cytokine profiles and disease severity during infection**

199 Due to the study design, recruitment was biased towards patients within the convalescent stage of
200 infection. Twenty-seven patients (23%) were recruited while being RT-PCR-positive, and three (3%)
201 became RT-PCR-positive after recruitment to CAPTURE. Cyto/chemokine profiling of 13 patients with
202 acute infection (8 solid tumour, 6 haematological malignancy) indicated that IL-6, IL-8 IFN- γ , IL-18, IL-
203 9, IP-10, and MIP1-Beta levels were elevated compared to control (**Extended Data Figure 1c,d, see**
204 **Methods**) and correlated with severe disease (**Extended Data Figure 1e,f**). Concentration of IFN- γ
205 and IL-18 in serum was significantly higher in patients with haematological malignancies¹⁸ (**Extended**
206 **Data Figure 1g**).

207

208 **S1-reactive SARS-CoV-2 antibody response in cancer patients**

209 We evaluated total S1-reactive antibody titres by ELISA at multiple time-points throughout the study
210 (with two median samples per patient [range: 1-10]). In total, 97/118 patients (82%) tested positive
211 (85/95 [89%] solid tumours, 12/21 [57%] haematological malignancy); blood samples were not
212 available for 2/118 patients (2%). Overall, 76/94 (81%) symptomatic and 21/24 (88%) asymptomatic
213 patients had S1-reactive antibodies, and among the symptomatic patients there was a non-

214 significant trend for higher S1-reactive antibody titres in those with higher COVID-19 severity ($P =$
215 0.057) (**Figure 2a**).

216 Thirteen patients (11%), with median follow up of 49 days (range: 14-344), had no evidence
217 of S1-reactive antibodies but were positive by SARS-CoV-2 RT-PCR. Six further patients without
218 detectable S1 antibody had no follow-up. Lack of seroconversion was significantly associated with
219 haematological malignancies: 9/21 patients (43%) with haematological vs 10/97 patients (10%) with
220 solid malignancies did not seroconvert ($p = 0.0012$). Antibody titres were also significantly lower in
221 patients with haematological malignancies (**Figure 2b**). Two patients with long COVID did not
222 seroconvert at any point during follow up.

223 A sensitive flow cytometric assay conducted on sera from a subset of patients with S1-
224 reactive antibodies ($n=40$; **Extended Data Figures 2a and 3**), detected S-specific IgG in 38/40 (95%)
225 (**Extended Data Figure 2b**) and IgM in 23/40 patients (58%) (**Extended Data Figure 2c**), with levels
226 significantly correlated with S1-reactive antibody titres ($P < 0.0001$) (**Extended Data Figure 2e-f**). S-
227 reactive IgA was detected in serum of only four patients (10%) (**Extended Data Figure 2d**), consistent
228 with the role of IgA in early response to SARS-CoV-2 infection.¹⁸

229 Finally, we evaluated matched pre-pandemic sera from 47 patients, 10 with and 37 without
230 S1-reactive antibodies in their sample collected during the pandemic. We found no evidence of S1-
231 reactive antibodies in the pre-pandemic sera in any patient (**Extended Data Figure 2g**), but S-
232 reactive IgG or IgM were detected in 18 patients without S1-reactive antibodies indicating cross-
233 reactivity to seasonal human coronaviruses.

234

235 **NABs against SARS-CoV-2 VOCs in cancer patients**

236 We next performed a live virus neutralisation assay to evaluate whether patients' sera could
237 neutralise SARS-CoV-2 (see **Methods**). We measured either neutralising activity against wild-type
238 (WT) SARS-CoV-2 or Alpha VOC, according to the causative variant (see **Methods**). We detected
239 neutralising antibody (NAb) activity in 84/97 patients (87%) with S1-reactive antibodies (75/85 [88%]
240 solid tumours, 8/12 [67%] haematological malignancy), with no significant differences in NAb titres
241 (NAbT) by COVID-19 severity (**Figure 2c**). NAbT against WT were significantly lower in patients with
242 haematological malignancies (**Figure 2d**). In a binary logistic regression model including all cancer
243 patients ($n=118$), presence of haematological malignancy, but not comorbidities, age, sex, or COVID-
244 19 severity was associated with lack of NAb (**Figure 2e**). In patients with solid tumours ($n=97$), there
245 was no association with cancer type, stage, progressive disease or cancer therapy (**Figure 2f,g**). We
246 were underpowered to evaluate patients with haematological malignancies ($n=21$), within a
247 multivariate model.

248 In a subset of NAb-positive patients (N=34, 31 with solid malignancies, 3 with
249 haematological malignancies; 25 with WT SARS-CoV-2 and 9 with Alpha VOC infection), we
250 compared NAb against WT, Alpha, Beta, and Delta. In patients with WT infection, overall lower
251 proportions of detectable responses (100% WT, 96% Alpha, 88% Beta, 85% Delta) were seen for VOC
252 as well as lower NAbT vs the WT strain (**Figure 2h**). Considering patients with Alpha VOC infection,
253 NAbT against Alpha VOC were increased vs WT and titres against Beta and Delta decreased vs. WT
254 and Alpha.

255 There was a significant correlation between S1-reactive and NAbT for all variants ($P < 0.01$)
256 (**Extended Data Figure 2h**); but we note that presence of S1-reactive antibodies was not always
257 predictive of neutralising response, especially to VOCs.

258

259 **SARS-CoV-2 antibody response lasts up to 11 months**

260 Next, we assessed antibody kinetics in 81/97 patients with S1-reactive antibodies and known
261 timing of POD (n=70 solid tumours, n=11 haematological malignancy). We analysed a median of two
262 timepoints per patient (range: 1-10) at a median follow-up of 56 days after POD (range: 1-344).
263 Seventy-seven (95%) had S1-reactive antibodies at the time of enrolment (median 51 days after
264 POD, range: 1-292, **Figure 2f**). Four patients (5%) had no antibodies at enrolment, but seroconverted
265 between day 13-117 days POD. S1-reactive antibody titres showed a weak declining trend and 12
266 patients (15%) became seronegative 24-321 days POD: one T-ALL patient who following COVID-19
267 had a stem cell transplant complicated by chronic graft-versus-host disease, and 11 solid tumour
268 patients with no unifying features to account for shorter-lived antibody response. Neutralising
269 antibodies were detected as early as day one (**Figure 2g**), and as late as day 292 after POD and
270 remained stable up to 329 days.

271

272 **SARS-CoV-2-specific T-cells are detected in cancer patients**

273 PBMC stimulation assays (see **Methods**) were performed in 104/118 SARS-CoV-positive
274 patients (n=83 solid tumour, n=21 haematological malignancy; **Extended Data Figure 3b**); 14
275 samples were excluded (for lack or low PBMC counts). SARS-CoV-2-specific CD4⁺ and CD8⁺ T-cells
276 (SsT-cells; identified by activation induced markers OX40, CD137, and CD69)¹⁹ were measured
277 (**Figure 3a,b**) at the first time point post-seroconversion (where evident), at the median of 54 days
278 after POD (range: 1-292). We detected CD4⁺ T-cells in 79/104 (76%), and CD8⁺ T-cells in 54/104
279 patients (52%) (**Figure 3c-f**). CD4⁺ T-cells were detected in 81% of patients with solid malignancies,
280 and in 41% of patients with haematological malignancies (**Figure 3c,e**). CD8⁺ T-cells were detected at
281 similar frequencies (53% and 48%) across both malignancy types (**Figure 3d,f**) at a level consistently

282 lower than CD4+ T-cells (**Extended Data Figure 4a**). The differences between CD8⁺ and CD4⁺ T-cell
283 responses may be due to using 15-mer peptide pools for stimulation, though we note similar
284 findings in non-cancer patients,^{20,21,22} indicating potential other factors, such as the broader range of
285 antigens that induce CD8⁺ T-cells compared to CD4⁺ T-cells.¹⁹

286 Consistent with functional activation, IFN- γ secreted by SsT-cells,²³ was detected after *in*
287 *vitro* stimulation, and IFN- γ concentrations correlated with the number of SsT-cells (**Extended Data**
288 **Figure 4b**).

289 Finally, as cross-reactive T-cell responses to HCoVs are observed frequently in healthy
290 individuals,^{19,24} and given the lack of matched pre-infection samples in our cohort, we extended the
291 T-cell assay to 12 cancer patients without confirmed SARS-CoV-2 infection. Cross-reactive CD4⁺ T-
292 cells were detected in 7/12 and CD8⁺ T-cells in 3/12 participants, though the overall proportion of
293 reactive T-cells was significantly lower than in patients with confirmed SARS-CoV-2 infection ($P < 0.05$)
294 (**Extended Data Figure 4c,d**).

295

296 **SsT-cell compensation in patients without humoral response**

297 Patients with haematological malignancies had a wide range of antibodies (**Figure 4a,b**) and SsT-cell
298 responses. In patients with leukaemia, NAb were detected in 6/11 and SsT-cells in 5/10 evaluable
299 patients (two had both CD4+ and CD8+, two had CD4+ only, and one had CD8+ only). In patients
300 with myeloma, 2/4 had NAb, and 3/4 had detectable SsT-cells (two both CD4+ and CD8+, one CD4+
301 only). None of the six lymphoma patients, including five who were treated with anti-CD20, had
302 detectable NAb, while SsT-cells were detected in 5/6 (three had both CD4+ and CD8+, one had
303 CD4+ only, and one had CD8+ only). One further patient with AML treated with anti-CD20 had
304 neither NAb nor SsT-cell responses. In total, we observed a discordance between antibody and T-cell
305 responses amongst patients with haematological malignancy, whereby 7/9 patients with NAb to
306 WT SARS-CoV-2 lacked SsT-cell response (CD4+ and/or CD8+), and in 12 patients without NAb
307 activity 7 had SsT-cell response. (**Figure 4c,d, Supplementary Table 3**). Overall, the levels of SsT-cells
308 were higher in patients with lymphomas vs leukaemias (**Figure 4e**). The highest levels of SsT-cells
309 was observed in a patient with diffuse large B-cell lymphoma and recent anti-CD20 therapy who had
310 no detectable neutralising antibodies.

311 In patients with solid malignancies, the level of SsT-cells did not differ significantly by
312 tumour type (**Figure 4f**) and the level of SARS-CoV-2-reactive CD4+ T-cells was positively correlated
313 with S1-reactive antibody titres (**Extended Data Figure 4e**), which was not observed in patients with
314 haematological malignancies (**Extended Data Figure 4f**). However, amongst 7/10 solid tumour
315 patients without NAb response, 5 had detectable SsT-cells (3 both CD4+ and CD8+, 2 CD4+ only,

316 **Supplementary Table 2**). Finally, following stimulation with S- and N- pools we observe that patients
317 with haematological malignancy exhibit higher level of N-reactive compared to S-reactive CD8+ T-
318 cells, (**Figure 4e,f**), while similar levels are observed in solid cancer patients (**Figure 4c,d**).

319

320 **T-cell responses are impacted in CPI-treated patients**

321 Next, we evaluated features associated with impaired T-cell responses to SARS-CoV-2 in
322 cancer patients. We found no association between lack of SsT-cells with the presence of solid or
323 haematological malignancies, nor with the number of comorbidities, age, sex, or COVID-19 severity
324 (**Figure 5a,b**). In patients with solid malignancies, those on CPI (n=14) had significantly reduced levels
325 of SARS-CoV-2 reactive CD4+ T-cells (**Figure 5e**), and in binary logistic regression model lack of SARS-
326 CoV-2 reactive CD4+ (but not CD8+) T-cells was associated with CPI therapy within three months of
327 SARS-CoV-2 infection (**Figure 5c,d**). Within the patients with haematological malignancies (n=21),
328 anti-CD20 (n=4) was not associated with obvious reduction of SARS-CoV-2 reactive T-cells (**Figure 5f**).

329 Discussion

330 Results from this prospective, longitudinal study of 118 SARS-CoV-2-positive cancer patients
331 indicated that most patients with solid tumours developed a functional and durable (at least 11
332 months) humoral immune response to SARS-CoV-2 infection, as well as an anti-SARS-CoV-2-specific
333 T-cell response. Patients with haematological malignancies had significantly lower seroconversion
334 rates, and impaired immune responses that were both disease- and treatment-related (anti-CD20),
335 although with evidence of compensation.

336 Most patients (82%) in our study had solid tumours and so findings largely reflect this cancer
337 population. The majority (89%) of solid cancer patients seroconverted following SARS-CoV-2
338 infection (as evidenced by the presence of S1-reactive antibodies). Delayed/lack of seroconversion
339 was observed in 10% of solid tumour patients, but no shared characteristics were identified among
340 them. The observed high seroconversion rates in solid tumour patients were in line with data
341 reported from smaller prospective studies conducted in the UK (95%, n=22)¹² and Italy (88%,
342 n=28);²⁵ in both those studies seroconversion rates were similar to those observed in individuals
343 without cancer. Recent studies in non-cancer subjects found a clear relationship between
344 neutralising responses and vaccine efficacy.^{26,27} We now showed that 88% of seroconverted solid
345 tumour patients also had functionally relevant NAb (against WT SARS-CoV-2 or Alpha, according to
346 the causative variant). Importantly, whilst we observed a weak decline in S1-reactive antibody titres,
347 NAbT were stable for up to 11 months of follow-up. In non-cancer population, inconsistent results
348 have been reported regarding the length of persistence of both SARS-CoV-2-specific IgG and NAb
349 over time,^{20,28-31} thus it is challenging to relate our data to those prior reports. In line with data for
350 non-cancer SARS-CoV-2 convalescent patients³², we found that neutralising activity against Alpha,
351 Beta, and Delta VOCs was decreased. This raises concerns about the ability of natural immunity to
352 one variant to protect against other VOCs. Given the majority of cancer patients would now have
353 been vaccinated against COVID-19, protection against evolving variants is critically relevant in the
354 context of COVID-19 vaccine-induced immunity (companion paper Fender *et al.*)

355 SARS-CoV-2-infected cancer patients were previously shown to have depleted T-cells which
356 showed markers of activation and exhaustion, and correlated with COVID-19 severity, but SsTcells
357 were not evaluated.¹² In our cohort, at a median of 54 days after POD, SsT-cells (including functional
358 IFN- γ expressing SsT-cells) were present in the majority of evaluated solid cancer patients (76%) and
359 in half of the haematological malignancy patients (52%). Both in the acute and convalescent phase
360 of SARS-CoV-2 infection, a significant proportion of SARS-CoV-2-specific CD4⁺ T-cells are T follicular
361 helper cells (Tfh)^{21,33} which are required for IgG and neutralising response by B-cells.³⁴ In our study,
362 the number of CD4⁺ T-cells was significantly correlated with S1-reactive antibody titres in solid

363 tumours, suggesting it may reflect Tfh T-cell activation and resulting B-cell activation. Overall, we
364 found no variables associating with impaired T-cell responses to SARS-CoV-2 in cancer patients,
365 except for CPI therapy within three months of SARS-CoV-2 infection (in solid tumours). It was
366 previously shown that PD-1 blockade during acute viral infection can increase viral clearance by
367 promoting CD8+ T-cell proliferation, but can also impair CD8+ T-cell memory differentiation, thereby
368 impairing long-term immunity.³⁵ While the role of PD-1 blockade on CD4+ T-cells during acute
369 infection is less well understood, PD-1 signalling regulates expansion of CD4+ T-cells upon an
370 immunogenic stimulus.³⁶

371 We found an inverse relationship between antibody and SsT-cell responses in patients with
372 haematological malignancies, whereby leukaemia patients had more pronounced antibody but
373 impaired SsT-cell responses, while the opposite was observed for lymphoma patients. Generally, in
374 patients with haematological malignancies immune responses were partially compensated, i.e. more
375 robust SsT-cell responses, especially CD8+ T-cell responses, were detected in patients without
376 antibody responses and vice versa. Furthermore, we found SsTcells in 4/5 evaluable patients on anti-
377 CD20 treatment, of whom none had humoral responses. In total, all but one patient with
378 haematological malignancies had mild or moderate disease, suggesting that SsT-cell responses,
379 specifically CD8+ T-cells and non-spike-specific SsT-cells, can at least partially compensate for lacking
380 humoral responses, although we note our cohort was largely convalescent. In one recent study,
381 10/13 patients with haematological malignancy and COVID-19 had SsT-cells, which were associated
382 with improved survival (including in those on anti-CD20 therapy).¹¹ Overall, the emerging data from
383 our study and others³⁷ appear to suggest that T-cell responses are likely important in those with
384 haematological malignancies and may offer protection from severe COVID-19 in the absence of
385 humoral responses.

386 The role of T-cells in protection from SARS-CoV-2 is not well understood, but T-cells were
387 shown to play a crucial role in the clearance of acute SARS-CoV infection in mice.³⁸ In line with this,
388 early induction of functional SsT-cells was demonstrated to associate with rapid viral clearance and
389 mild disease in COVID-19 patients,³⁹ and preclinical animal studies suggest a role for cellular
390 immunity in SARS-CoV-2 clearance.⁴⁰ Importantly, SsTcells were shown to be induced by COVID-19
391 vaccines in both non-cancer^{41,42} and cancer (companion paper Fender *et al.*) population, and to have
392 activity against VOCs.⁴³ Furthermore, VOCs are not expected to escape SsTcell responses due to
393 their highly multi-antigenic and multi-specific properties.⁴³ In the general population, data indicate
394 that SARS-CoV-2-specific memory T-cells are maintained beyond eight months following
395 infection.^{20,44} In the context of the outbreak of SARS in 2003, SARS-specific T-cells were detected up
396 to 17 years after infection, much longer than antibodies.⁴⁵ An ongoing aim of the CAPTURE study is

397 to evaluate the nature, durability, and clinical correlates of SsT-cell response in cancer patients as
398 the pandemic evolves, especially in the context of COVID-19 vaccines.

399 This report has several limitations. Firstly, lack of a matched non-cancer cohort prevents
400 direct comparisons between populations with and without cancer. Secondly, as mentioned above,
401 the way patients are recruited into CAPTURE, including in the course of routine clinical care, may
402 introduce selection bias, and thus our findings may not be fully generalizable to the wider cancer
403 population. The fact that we recorded only two COVID-19-related deaths may be reflective of this (as
404 well as the relatively low proportion of lung and haematological malignancies – the two cancer
405 groups with increased COVID-19-related mortality).³⁻⁶ Furthermore, all but one patient with
406 haematological malignancies in our cohort recovered, while 11/18 patients with blood cancers died
407 due to COVID-19 at our institution⁴⁶ before enrolment into CAPTURE commenced. Thus, it is possible
408 that the patients with haematological malignancy in our analysis are not entirely representative of
409 this population. Additional limitation pertains to our SsT-cell assessment - this was performed at a
410 single time-point and so in instances where we did not detect a response, this might represent a
411 timing bias rather than a lack of capacity to develop a response *per se*. As recruitment to CAPTURE
412 commenced in May 2020 - which marked the end of the first wave of SARS-CoV-2 infections in the
413 UK - most of the initially recruited participants were infected prior to study enrolment and evaluated
414 in the convalescent phase. Even with the contribution of acutely infected patients recruited chiefly
415 during the second wave, this analysis mainly assesses the immune protective response and its
416 durability. Finally, some of the sub-group analyses are likely to be underpowered to robustly detect
417 differences in immune response.

418 In summary, our data suggest that patients with solid malignancies are capable of
419 developing humoral and cellular immunity against SARS-CoV-2, with NAb detectable for up to 11
420 months. In line with others,^{11,12} we found that patients with haematological malignancies had
421 impaired humoral response, which was associated with malignancy type and anti-CD20 treatments,
422 but was often linked to detectable SsT-cell responses. Finally, we found that neutralising activity
423 against VOCs was reduced in samples from patients infected with WT SARS-CoV-2, which raises
424 concerns about the effectiveness of naturally acquired immune responses against new SARS-CoV-2
425 VOCs. Whether such response can be boosted by COVID-19 vaccines remains under investigation in
426 the vaccine cohort of CAPTURE, including the currently predominant Delta VOC (companion paper
427 Fender *et al.*).

428 **Methods**

429 **Study design**

430 CAPTURE (NCT03226886) is a prospective, longitudinal cohort study that commenced recruitment in
431 May 2020 at the Royal Marsden NHS Foundation Trust. The study design has been previously
432 published.¹⁴ In brief, adult patients with current or history of invasive cancer are eligible for
433 enrolment (**Figure 1A**). Inclusion criteria are intentionally broad, and patients are approached
434 irrespective of cancer type, stage, or treatment. Patients with confirmed or suspected SARS-CoV-2
435 infection are targeted with broader recruitment in the course of routine clinical care (asymptomatic
436 cases). Patients are screened at each study visit and classified as SARS-CoV-2-negative or SARS-CoV-
437 2-positive based on a laboratory case definition of RT-PCR positive result and/or S1-reactive
438 antibodies (details below). The primary endpoint is to describe the population characteristics of
439 SARS-CoV-2 positive and negative cancer patients. The secondary endpoints include the impact of
440 COVID-19 on long-term survival and ICU admission rates. Exploratory endpoints pertain to
441 characterising clinical and immunological determinants of COVID-19 in cancer patients.

442

443 CAPTURE was approved as a substudy of TRACERx Renal (NCT03226886). TRACERx Renal was initially
444 approved by the NRES Committee London, Fulham, on January 17, 2012. The TRACERx Renal sub-
445 study CAPTURE was submitted as part of Substantial Amendment 9 and approved by the Health
446 Research Authority on April 30, 2020 and the NRES Committee London - Fulham on May 1, 2020.
447 CAPTURE is being conducted in accordance with the ethical principles of the Declaration of Helsinki,
448 Good Clinical Practice and applicable regulatory requirements. All patients provided written
449 informed consent to participate.

450

451 **Study schedule and follow-up**

452 Clinical data and sample collection for participating cancer patients is performed at baseline, and at
453 clinical visits per standard-of-care management during the first year of follow-up; frequency varies
454 depending on in- or outpatient status and systemic anti-cancer treatment regimens. For inpatients,
455 study assessments are repeated every 2-14 days. For outpatients, the follow-up study assessments
456 are aligned with clinically indicated hospital attendances. The frequency of study assessments in the
457 first year for patients on anti-cancer therapies are as follows: every cycle for immune checkpoint
458 inhibitors or targeted therapies; every second cycle for chemotherapy; every outpatient
459 appointment (maximum 6 weekly) for patients on endocrine therapy or in surveillance or routine
460 cancer care follow-up. Patient reported data is collected 3-monthly via an online questionnaire. In

461 year two to five of follow-up, the frequency of study assessments is reduced (see **Supplementary**
462 **Material Study Protocol**).

463 **Data and Sample Sources**

464 Patient-reported outcome data are collected using PROFILES (Patient Reported Outcomes Following
465 Initial treatment and Long-term evaluation of Survivorship; <https://profiles-study.rmh.nhs.uk/>).
466 PROFILES is a web-based questionnaire administration and management system designed for the
467 study of the physical and psychosocial impact of cancer and its treatment. Online questionnaires for
468 baseline and follow up assessments were designed to record data for cancer patients participating in
469 CAPTURE. Collected self-reported data include: ethnicity, smoking status, alcohol consumption,
470 recent travel history, occupation, exercise habits, dietary habits, previous medical history,
471 autoimmune disease (self, next of kin), vaccination history, concomitant medication, self-shielding
472 status, previous SARS-CoV-2 tests, SARS-CoV-2 tests in household members, current and recent
473 symptoms. Further demographic, epidemiological and clinical data (e.g. cancer type, cancer stage,
474 treatment history) are collected from the internal electronic patient record system and entered into
475 detailed case report forms in a secure electronic database. For information on anti-cancer
476 intervention and response to most recent anti-cancer intervention, data was collected reflective of
477 the time of SARS-CoV-2 infection per definition above where available, or the time of enrolment if
478 data of disease onset is unknown (e.g. asymptomatic infections defined by positive serological
479 positivity but negative/no RT-PCR results).

480 Study samples collected comprise blood samples, oropharyngeal swabs and archival and excess
481 material from routine clinical investigations. Detailed sampling schedule and methodology has been
482 previously described.¹⁴ Surplus serum from patient biochemistry samples taken as part of routine
483 care were also retrieved and linked to the study IDs before anonymisation and study analysis.
484 Collected data and study samples are de-identified and stored with only the study-specific study
485 identification number. For self-reported data, a PROFILES member number is used, which is
486 generated automatically.

487 **WHO classification of severity of COVID-19**

488 We classified severity of COVID-19 according to the WHO clinical progression scale.⁴⁷ Uninfected:
489 uninfected, no viral RNA detected - 0; Asymptomatic: viral RNA and/or S1-reactive IgG detected – 1;
490 mild (ambulatory): symptomatic, independent – 2; symptomatic, assistance needed - 3; moderate
491 (hospitalised): no oxygen therapy (if hospitalised for isolation only, record status as for ambulatory
492 patient) – 4; oxygen by mask or nasal prongs - 5; severe (hospitalised): oxygen by non-invasive
493 ventilation or high flow – 6; intubation and mechanical ventilation, pO₂/FiO₂ ≥ 150 or SpO₂/FiO₂ ≥

494 200 – 7; mechanical ventilation, pO₂/FiO₂ < 150 (SpO₂/FiO₂ < 200) or vasopressors – 8; mechanical
495 ventilation, pO₂/FiO₂ < 150 and vasopressors, dialysis, or extracorporeal membrane oxygenation - 9;
496 Dead - 10.

497 **Cell lines and viruses**

498 SUP-T1 cells stably transfected with spike or control vectors were obtained from M.P., and L.M.i.
499 Vero E6 cells were from the National Institute for Biological Standards and Control, UK. The SARS-
500 CoV-2 isolate hCoV-19/England/02/2020 was obtained from the Respiratory Virus Unit, Public Health
501 England, UK, and propagated in Vero E6 cells.

502 **Handling of oronasopharyngeal swabs, RNA isolation and RT-PCR**

503 SARS-CoV-2 RT-PCR was performed from oronasopharyngeal (ONP) swabs using a diagnostics assay
504 established at the Francis Crick Institute. The complete standard operating procedure is available on
505 the Crick Covid-19 consortium website: [https://www.crick.ac.uk/research/covid-19/covid19-](https://www.crick.ac.uk/research/covid-19/covid19-consortium)
506 [consortium](https://www.crick.ac.uk/research/covid-19/covid19-consortium). ONP swabs were collected in VTM medium, frozen within 24 hrs after collection, and
507 stored at -80°C until processing. ONP swabs were handled in a CL3 laboratory inside a biosafety
508 cabinet using appropriate personal protective equipment and safety measures, which were in
509 accordance with a risk assessment and standard operating procedure approved by the safety, health
510 and sustainability committee at the Francis Crick Institute. In brief, 100 µl of swab vial content was
511 inactivated in 5 M Guanidinium thiocyanate and RNA isolated using a completely automated kit-free,
512 silica bead-based method.

513 PCR detection of SARS-CoV-2 was performed from 10 µl extracted RNA using two kits depending on
514 the date of test. Up to 6th December 2020, samples were tested in duplicate using Real-Time
515 Fluorescent RT-PCR Kit for Detecting 2019-nCoV (BGI). Positive, negative, and extraction controls
516 were included on each plate. Runs were regarded as valid when negative control Ct values were >37
517 and positive controls when Ct values were <37. Samples were only considered positive if Ct values in
518 both replicates were <37. From 7th December 2020, tests were performed using TaqPath COVID-19
519 CE-IVD RT-PCR Kit (Thermo Fisher), this time without replicate. Positive and negative controls were
520 included on each plate and samples reported positive if 2 or 3 SARS-CoV-2 targets had Ct value <37
521 and the internal control Ct <32. With both kits, samples with non-exponential amplification were
522 excluded from analysis.

523 **Viral Sequencing**

524 All PCR-positive samples with ORF1ab Ct value < 32 were selected for viral sequencing, representing
525 52 samples from 32 patients. Sequencing was performed either on Illumina or on Oxford Nanopore

526 Technologies instruments. Oxford Nanopore libraries were prepared following the ARTIC nCoV-2019
527 sequencing protocol v3 (LoCost) (protocols.io[https://protocols.io/view/ncov-2019-sequencing-
528 protocol-v3-locost-bh42j8ye](https://protocols.io/view/ncov-2019-sequencing-protocol-v3-locost-bh42j8ye)) and then sequenced for 20 hours on a MinION flowcell on a GridION
529 instrument. The ncov2019-artic-nf pipeline (version v1.1.1; [https://github.com/connor-
530 lab/ncov2019-artic-nf](https://github.com/connor-lab/ncov2019-artic-nf)) written in the Nextflow domain specific language (version 20.10.0)⁴⁸ was used
531 to perform the QC, variant calling and consensus sequence generation for the samples. The full
532 command used was "nextflow run ncov2019-artic-nf --nanopolish --prefix \$PREFIX --basecalled_fastq
533 fastq_pass/ --fast5_pass fast5_pass/ --sequencing_summary sequencing_summary.txt --
534 schemeVersion V3 --minReadsPerBarcode 1 --minReadsArticGuppyPlex 1 -with-singularity artic-
535 ncov2019-nanopore.img -profile singularity,slurm -r v1.1.1". Illumina libraries were prepared
536 following the CoronaHiT protocol with minor modifications⁴⁹, pooled and then sequenced at 100bp
537 paired end on HiSeq 4000. The nf-core/viralrecon pipeline (version 1.1.0)⁵⁰ was used to perform the
538 QC, variant calling and consensus sequence generation for the samples. The full command used was
539 "nextflow run nf-core/viralrecon --input samplesheet.csv --genome 'MN908947.3' --amplicon_bed
540 nCoV-2019.artic.V3.bed --protocol 'amplicon' --callers ivar --skip_assembly --skip_markduplicates --
541 skip_fastqc --skip_picard_metrics --save_align_intermeds -profile crick -r 1.1.0". 44/52 passed
542 quality control (>50% consensus sequence) and lineage was obtained using PANGOLIN
543 (<https://github.com/cov-lineages/pangolin>). In the absence of sequencing data to confirm the
544 causative SARS-CoV-2 variant, all patients tested with ThermoFisher TaqPath RT-PCR kit that
545 reported S-dropout were considered to be infected with Alpha VOC.

546 **Viral shedding**

547 Duration of viral shedding was estimated from research and opportunistic swabs and was defined as
548 the time from first positive swab to the last positive swab (preceded by at least one negative swab).

549 **Handling of whole blood samples**

550 All blood samples and isolated products were handled in a CL2 laboratory inside a biosafety cabinet
551 using appropriate personal protective equipment and safety measures, which were in accordance
552 with a risk assessment and standard operating procedure approved by the safety, health and
553 sustainability committee of the Francis Crick Institute. For indicated experiments, serum or plasma
554 samples were heat-inactivated at 56°C for 30 minutes prior to use after which they were used in a
555 CL1 laboratory.

556 **Plasma and PBMC isolation**

557 Whole blood was collected in EDTA tubes (VWR) and stored at 4°C until processing. All samples were
558 processed within 24 hours. Time of blood draw, processing, and freezing was recorded for each
559 sample. Prior to processing tubes were brought to room temperature (RT). PBMC and plasma were
560 isolated by density-gradient centrifugation using pre-filled centrifugation tubes (pluriSelect). Up to
561 30 ml of undiluted blood was added on top of the sponge and centrifuged for 30 minutes at 1000g at
562 RT. Plasma was carefully removed then centrifuged for 10 minutes at 4000g to remove debris,
563 aliquoted and stored at -80°C. The cell layer was then collected and washed twice in PBS by
564 centrifugation for 10 minutes at 300 x g at RT. PBMC were resuspended in Recovery cell culture
565 freezing medium (Fisher Scientific) containing 10% DMSO, placed overnight in CoolCell freezing
566 containers (Corning) at -80°C and then stored at -80°C.

567 **Serum isolation**

568 Whole blood was collected in serum coagulation tubes (Vacuette CAT tubes, Greiner) for serum
569 isolation and stored at 4°C until processing. All samples were processed within 24 hrs. Time of blood
570 draw, processing, and freezing was recorded for each sample. Tubes were centrifuged for 10
571 minutes at 2000 x g at 4°C. Serum was separated from the clotted portion, aliquoted and stored at -
572 80°C.

573 **S1-reactive IgG ELISA**

574 Ninety-six-well MaxiSorp plates (Thermo Fisher Scientific) were coated overnight at 4°C with purified
575 S1 protein in PBS (3 µg/ml per well in 50 µl) and blocked for 1 hour in blocking buffer (PBS, 5% milk,
576 0.05% Tween 20, and 0.01% sodium azide). Sera were diluted in blocking buffer (1:50). Fifty
577 microliters of serum were added to the wells and incubated for 2 hours at RT. After washing
578 four times with PBS-T (PBS, 0.05% Tween 20), plates were incubated with alkaline phosphatase-
579 conjugated goat anti-human IgG (1:1000, Jackson ImmunoResearch) for 1 hour. Plates were
580 developed by adding 50 µl alkaline phosphatase substrate (Sigma Aldrich) for 15-30 minutes after six
581 washes with PBS-T. Optical densities were measured at 405 nm on a microplate reader (Tecan).
582 CR3022 (Absolute Antibodies) was used as a positive control. The cut-off for a positive response was
583 defined as the mean negative value multiplied by 0.35 times the mean positive value.

584 **Flow cytometry for spike-reactive IgG, IgM, and IgA**

585 SUP-T1 cells were harvested, counted and spike-expressing and control SUP-T1 cells were mixed in a
586 1:1 ratio. The cell mix was transferred into V-bottom 96-well plates at 20,000 cells per well. Cells
587 were incubated with heat-inactivated sera diluted 1:50 in PBS for 30 minutes, washed with FACS
588 buffer (PBS, 5% BSA, 0.05% sodium azide), and stained with FITC anti-IgG (clone HP6017, Biolegend),

589 APC anti-IgM (clone MHM-88, Biolegend) and PE anti-IgA (clone IS11-8E10, Miltenyi Biotech) for 30
590 minutes (all antibodies diluted 1:200 in FACS buffer). Cells were washed with FACS buffer and fixed
591 for 20 minutes in 1% PFA in FACS buffer. Samples were run on a Bio-Rad Ze5 analyser running Bio-
592 Rad Everest software v2.4 and analysed using FlowJo v10.7.1 (Tree Star Inc.) analysis software.
593 Spike-expressing and control SUP-T1 cells were gated and mean fluorescence intensity (MFI) of both
594 populations was measured. MFI in control SUP-T1 cells was subtracted from MFI in spike-expressing
595 SUP-T1 cells, and resulting values were divided by MFI in control SUP-T1 cells to calculate the
596 specific increase in MFI. Values >2 were considered positive.

597 **Neutralising antibody assay against SARS-CoV-2**

598 Confluent monolayers of Vero E6 cells were incubated with SARS-CoV-2 WT or Alpha virus and two-
599 fold serial dilutions of heat-treated serum or plasma samples starting at 1:40 for 4 hrs at 37°C, 5%
600 CO₂, in duplicates. The inoculum was then removed and cells were overlaid with viral growth
601 medium. Cells were incubated at 37°C, 5% CO₂. At 24 hours post-infection, cells were fixed in 4%
602 paraformaldehyde and permeabilized with 0.2% Triton X-100/PBS. Virus plaques were visualized by
603 immunostaining, as described previously for the neutralisation of influenza viruses using a rabbit
604 polyclonal anti-NSP8 antibody used at 1:1000 dilution and anti-rabbit-HRP conjugated antibody at
605 1:1000 dilution and detected by action of HRP on a tetramethyl benzidine-based substrate. Virus
606 plaques were quantified and ID₅₀ was calculated.

607 **High-throughput live virus microneutralisation assay**

608 High-throughput live virus microneutralisation assays were performed for a subset of 37 patients for
609 WT SARS-CoV-2, Alpha, Beta or Delta. High-throughput live virus microneutralisation assays were
610 performed as described previously.⁵¹ Briefly, Vero E6 cells (Institute Pasteur) or Vero E6 cells
611 expressing ACE2 and TMPRSS2 (VAT-1) (Centre for Virus Research)⁵² at 90-100% confluency in 384-
612 well format were first titrated with varying MOI of each SARS-CoV-2 variant and varying
613 concentrations of a control monoclonal nanobody in order to normalise for possible replicative
614 differences between variants and select conditions equivalent to wild-type virus. Following this
615 calibration, cells were infected in the presence of serial dilutions of patient serum samples. After
616 infection (24 hrs Vero E6 Pasteur, 16hrs VAT-1), cells were fixed with 4% final Formaldehyde,
617 permeabilised with 0.2% TritonX-100, 3% BSA in PBS (v/v), and stained for SARS-CoV-2 N protein
618 using Alexa488-labelled-CR3009 antibody produced in-house and cellular DNA using DAPI7. Whole-
619 well imaging at 5x was carried out using an Opera Phenix (Perkin Elmer) and fluorescent areas and
620 intensity calculated using the Phenix-associated software Harmony 9 (Perkin Elmer). Inhibition was
621 estimated from the measured area of infected cells/total area occupied by all cells. The inhibitory

622 profile of each serum sample was estimated by fitting a 4-parameter dose response curve executed
623 in SciPy. Neutralising antibody titres are reported as the fold-dilution of serum required to inhibit
624 50% of viral replication (IC₅₀), and are further annotated if they lie above the quantitative (complete
625 inhibition) range, below the quantitative range but still within the qualitative range (i.e. partial
626 inhibition is observed but a dose- response curve cannot be fit because it does not sufficiently span
627 the IC₅₀), or if they show no inhibition at all. IC₅₀ values above the quantitative limit of detection of
628 the assay (>25600) were recoded as 3000; IC₅₀ values below the quantitative limit of the assay (< 40)
629 but within the qualitative range were recoded as 39 and data below the qualitative range (i.e. no
630 response observed) were recoded as 35.

631 **PBMC stimulation assay**

632 PBMC for in vitro stimulation were thawed at 37 °C and resuspended in 10 ml of warm complete
633 medium (RPMI, 5% human AB serum) containing 0.02% benzonase. Viable cells were counted and
634 1x10⁶ to 2x10⁶ cells were seeded in 200 µl complete medium per well of a 96-well plate. Cells were
635 stimulated with 4 µl/well PepTivator SARS-CoV-2 spike (S), membrane (M), or nucleocapsid (N) pools
636 (i.e., synthetic SARS-CoV-2 peptide pools, consisting of 15-mer sequences with 11 amino acid
637 overlap covering the immunodominant parts of the S protein and the complete sequence of the N
638 and membrane M proteins), representing 1µg/ml final concentration per peptide (Miltenyi Biotec,
639 Surrey, UK). Staphylococcal enterotoxin B (Merck, UK) was used as a positive control at 0.5µg/ml
640 final concentration, negative control was PBS containing DMSO at 0.002% final concentration. PBMC
641 were cultured for 24 hrs at 37°C, 5% CO₂.

642 **Activation-induced marker assay**

643 PBMC supernatants were collected for cytokine analysis after stimulation for 24 hours. Cells were
644 washed twice in warm PBMC. Dead cells were stained with 0.5 µl/well Zombie dye V500 for 15
645 minutes at RT in the dark, then washed once with PBS containing 2% FCS (FACS buffer). A surface
646 staining mix was prepared per well, containing 2 µl/well of each antibody for surface staining (see
647 **key resources table** for a full list of antibodies) in 50:50 brilliant stain buffer (BD) and FACS buffer.
648 PBMC were stained with 50 µl surface staining mix per well for 30 minutes at RT in the dark. Cells
649 were washed once in FACS buffer and fixed in 1% PFA in FACS buffer for 20 min, then washed once
650 and resuspended in 200 µl PBS. All samples were acquired on a Bio-Rad Ze5 flow cytometer running
651 Bio-Rad Everest software v2.4 and analysed using FlowJo v10.7.1 (Tree Star Inc.) analysis software.
652 Compensation was performed with 20 µl antibody-stained anti-mouse Ig, k / negative control
653 compensation particle set (BD Biosciences, UK). 1x10⁶ live CD19-/CD14- cells were acquired per
654 sample. Gates were drawn relative to the unstimulated control for each donor. T-cell response is

655 displayed as a stimulation index by dividing the percentage of AIM-positive cells by the percentage
656 of cells in the negative control. If negative control was 0 the minimum value across the cohort was
657 used. When S, M, and N stimulation were combined the sum of AIM-positive cells was divided by
658 three times the percentage of positive cells in the negative control. A 1.5-fold increase in stimulation
659 index is considered positive.

660 **IFN- γ ELISA**

661 IFN- γ ELISA was performed using the human IFN- γ DuoSet ELISA (R&D Systems) according to the
662 manufacturer's instructions. Briefly, 96-well plates were coated overnight with capture antibody,
663 washed twice in wash buffer then blocked with reagent diluent for 2 hrs at RT. 100 μ l of PBMC
664 culture supernatants were added and incubated for 1 hr at RT and washed twice in wash buffer. 100
665 μ l detection antibody diluted in reagent diluent was added per well and incubated for 2 hrs at RT.
666 Plates were washed twice in wash buffer. 100 μ l streptavidin-HRP dilution was added to the plates
667 and incubated for 20 minutes in the dark at RT, plates were washed twice in wash buffer. The
668 reaction was developed using 200 μ l substrate solution for 20 minutes in the dark at RT then
669 stopped with 50 μ l stop solution. Optical density was measured at 450 nm on a multimode
670 microplate reader (Berthold). Serial dilutions of standard were run on each plate. Concentrations
671 were calculated by linear regression of standard concentrations ranging 0-600 pg/ml and normalized
672 to the number of stimulated PBMC. The assay sensitivity was 5 pg/ml.

673 **Multiplex immune assay for cytokines and chemokines**

674 The preconfigured multiplex Human Immune Monitoring 65-plex ProcartaPlex immunoassay kit
675 (Invitrogen, Thermo Fisher Scientific, UK) was used to measure 65 protein targets in plasma on the
676 Bio-Plex platform (Bio-Rad Laboratories, Hercules, CA, USA), using Luminex xMAP technology.
677 Analytes measured included APRIL; BAFF; BLC; CD30; CD40L; ENA-78; Eotaxin; Eotaxin-2; Eotaxin-3;
678 FGF-2; Fractalkine; G-CSF; GM-CSF; Gro-Alpha; HGF; IFN-Alpha; IFN-gamma; IL-10; IL-12p70; IL-13; IL-
679 15; IL-16; IL-17A; IL-18; IL-1Alpha; IL-1Beta; IL-2; IL-20; IL-21; IL-22; IL-23; IL-27; IL-2R; IL-3; IL-31; IL-4;
680 IL-5; IL-6; IL-7; IL-8; IL-9; IP-10; I-TAC; LIF; MCP-1; MCP-2; MCP-3; M-CSF; MDC; MIF; MIG; MIP-
681 1Alpha; MIP-1Beta; MIP-3Alpha; MMP-1; NGF-Beta; SCF; SDF-1Alpha; TNF-Beta; TNF-Alpha; TNF-R2;
682 TRAIL; TSLP; TWEAK; VEGF-A. All assays were conducted as per the manufacturer's
683 recommendation.

684 **Statistics & Reproducibility**

685 No statistical method was used to predetermine sample size but as many patients with SARS-CoV-2
686 infection were recruited as possible including patients with no history of infection to identify

687 patients in routine care with asymptomatic infection. The experiments were not randomised. The
688 investigators were not blinded to allocation during experiments and outcome assessment.

689 Data and statistical analysis were done in FlowJo 10 and R v3.6.1 in R studio v1.2.1335. Gaussian
690 distribution of baseline characteristics was tested by Kolmogorov-Smirnov test and differences in
691 patient groups were compared using Chi-squared test, Mann-Whitney or Kruskal-Wallis tests as
692 appropriate. Statistical methods for each experiment are provided in the figure legends. Gaussian
693 distribution was tested by Kolmogorov-Smirnov test. Mann-Whitney, Wilcoxon, Kruskal-Wallis, Chi²,
694 Fisher's exact test, and Friedman tests were performed for statistical significance. A p-value <0.05
695 was considered significant. The ggplot2 package in R was used for data visualization and illustrative
696 figures were created with BioRender.com. Data are usually plotted as single data points and box
697 plots on a logarithmic scale. For boxplots, boxes represent upper and lower quartiles, line represents
698 median, and whiskers IQR times 1.5. Notches represent confidence intervals of the median. For
699 correlation matrix analysis, spearman rank correlation coefficients were calculated between all
700 parameter pairs using the corplot package in R without clustering. For pairwise correlation
701 spearman rank correlation coefficients were calculated. Multivariate binary logistic regression
702 analysis was performed using the glm function with the stats package in R.

703 **Reporting Summary**

704 Further information on research design is available in the Nature Research Reporting Summary
705 linked to this article.

706 **Data availability**

707 All requests for raw and analysed data, and CAPTURE study protocol will be reviewed by the
708 CAPTURE Trial Management Team, Skin and Renal Clinical Trials Unit, The Royal Marsden NHS
709 Foundation Trust (CAPTURE@rmh.nhs.uk) to determine if the request is subject to confidentiality
710 and data protection obligations. Materials used in this study will be made available upon request.
711 There are restrictions to the availability based on limited quantities. Response to any request for
712 data and/or materials will be given within a 28 day period. Data and materials that can be shared
713 would then be released upon completion of a material transfer agreement.

714 **Code availability**

715 No unpublished code was used in this study.

716 **Acknowledgements**

717 We thank the CAPTURE trial team, including Eleanor Carlyle, Kim Edmonds, and Lyra Del Rosario, as
718 well as Somya Agarwal, Hamid Ahmod, Natalie Ash, Ravinder Dhaliwal, Lauren Dowdie, Tara Foley,
719 Lucy Holt, Dilruba Kabir, Molly O’Flaherty, Mandisa Ndlovu, Sonia Ali, Justine Korteweg, Charlotte
720 Lewis, Karla Lingard, Mary Mangwende, Aida Murra, Kema Peat, Sarah Sarker, Nahid Shaikh, Sarah
721 Vaughan, and Fiona Williams. We acknowledge the tremendous support from the clinical and
722 research teams at participating units at the Royal Marsden Hospital, including Ethel Black, Arnold
723 Dela Rosa, Carole Pearce, Jessica Bazin, Leonora Conneely, Chloe Burrows, Tommy Brown, Jeremy
724 Tai, Emma Lidington, Holly Hogan, Amanda Upadhyay, David Capdeferro, Ingrid Potyka, Annette
725 Drescher, Farzana Baksh, Melissa Balcorta, Catia Da Costa Mendes, Joao Amorim, Venus Orejudos,
726 and Louise Davison. We also thank the Volunteer Staff at The Francis Crick Institute, the Crick
727 COVID19 consortium, Alice Lilley for help with neutralising assays, Antonia Toncheva, and the
728 cloning unit at Autolus including James Sillibourne, Katarzyna Ward, Katarina Lamb and Philip Wu.
729 We thank Brigitta Stockinger for her thoughtful review and comments on the manuscript. Due to the
730 pace at which the field is evolving, we acknowledge researchers in COVID-19, particularly in
731 furthering our understanding of SARS-CoV-2 infection and we apologise for work that was not cited.
732 This research was funded in part, by the Cancer Research UK (grant reference number
733 C50947/A18176). This work was supported by the Francis Crick Institute, which receives its core
734 funding from Cancer Research UK (CRUK) (FC001988, FC001218, FC001099, FC001002, FC001078,
735 FC001169, FC001030), the UK Medical Research Council (FC001988, FC001218, FC001099,
736 FC001002, FC001078, FC001169, FC001030), and the Wellcome Trust (FC001988, FC001218,
737 FC001099, FC001002, FC001078, FC001169, FC001030). For the purpose of Open Access, the author
738 has applied a CC BY public copyright licence to any Author Accepted Manuscript version arising from
739 this submission. TRACERx Renal is partly funded by the National Institute for Health Research (NIHR)
740 Biomedical Research Centre (BRC) at the Royal Marsden Hospital and Institute of Cancer Research
741 (ICR) (A109). The CAPTURE study is sponsored by The Royal Marsden NHS Foundation Trust and
742 funded from a grant from The Royal Marsden Cancer Charity. A.F. has received funding from the
743 European Union’s Horizon 2020 research and innovation programme under the Marie Skłodowska-
744 Curie grant agreement No. 892360. L.A. is funded by the Royal Marsden Cancer Charity. S.T. is
745 funded by Cancer Research UK (grant reference number A29911); the Francis Crick Institute, which
746 receives its core funding from Cancer Research UK (FC10988), the UK Medical Research Council

747 (FC10988), and the Wellcome Trust (FC10988); the National Institute for Health Research (NIHR)
748 Biomedical Research Centre at the Royal Marsden Hospital and Institute of Cancer Research (grant
749 reference number A109), the Royal Marsden Cancer Charity, The Rosetrees Trust (grant reference
750 number A2204), Ventana Medical Systems Inc (grant reference numbers 10467 and 10530), the
751 National Institute of Health ((U01 CA247439) and Melanoma Research Alliance (Award Ref no
752 686061). C.S. is Royal Society Napier Research Professor (RP150154). His work is supported by the
753 Francis Crick Institute, which receives its core funding from Cancer Research UK (FC001169), the UK
754 Medical Research Council (FC001169), and the Wellcome Trust (FC001169). C.S. is funded by Cancer
755 Research UK (TRACERx, PEACE and CRUK Cancer Immunotherapy Catalyst Network), Cancer
756 Research UK Lung Cancer Centre of Excellence, the Rosetrees Trust, Butterfield and Stoneygate
757 Trusts, NovoNordisk Foundation (ID16584), Royal Society Research Professorship Enhancement
758 Award (RP/EA/180007), the NIHR BRC at University College London Hospitals, the CRUK-UCL Centre,
759 Experimental Cancer Medicine Centre and the Breast Cancer Research Foundation, USA (BCRF). His
760 research is supported by a Stand Up To Cancer-LUNGevity-American Lung Association Lung Cancer
761 Interception Dream Team Translational Research Grant (SU2C-AACR-DT23-17). Stand Up To Cancer
762 is a program of the Entertainment Industry Foundation. Research grants are administered by the
763 American Association for Cancer Research, the Scientific Partner of SU2C. C.S. also receives funding
764 from the European Research Council (ERC) under the European Union's Seventh Framework
765 Programme (FP7/2007-2013) Consolidator Grant (FP7-THESEUS-617844), European Commission ITN
766 (FP7-PloidyNet 607722), an ERC Advanced Grant (PROTEUS) from the European Research Council
767 under the European Union's Horizon 2020 research and innovation programme (835297) and
768 Chromavision from the European Union's Horizon 2020 research and innovation programme
769 (665233). R.W. has received Francis Crick Institute supported by Wellcome (FC0010218), UKRI
770 (FC0010218), CRUK (FC0010218) and research funding from Wellcome (203135 and 222754),
771 Rosetrees (M926) and The South African MRC.

772 **Author contributions**

773 Conceptualisation, S.T., L.A. and L.A.B.; Methodology, S.T., A.Fendler, F.B., K.A.W., G.K. and R.H.
774 Software, M.G.; Formal Analysis, A.Fendler., L.A., S.T.C.S., G.K., K.W., R.W., R.H. and M.C.;
775 Investigation, A.F., L.A., F.B., S.T.C.S, B.S., C.G., W.X., B.W., K.W., M.C., A.A-D. and R.H.; Resources,
776 S.T., A.Fendler, L.A., L.A.B., F.B., S.T.C.S., B.S., C.G., B.W., W.X., M.C., G.C., M.P. and L.M., R.S., C.G.,
777 H.F., M.G., F.G., O.C., T.S., Y.K., Z.T. and I.L.; Data Curation, L.A.B., S.T.C.S, B.S., C.G., A.Fendler and
778 L.A.; Writing – Original Draft: S.T., K.R., A.Fendler, L.A., S.T.C.S.; Writing - Review & Editing: All;

779 Visualization, A.Fendler, S.T.C.S, S.T. and L.A.; Supervision, S.T.; Trial conduct, S.T., L.A., S.T.C.S, E.C.,
780 L.R., K.E., L.A.B., J.L., N.Y., A.R., E.N. and S.K.

781 **Competing interests**

782 ST has received speaking fees from Roche, Astra Zeneca, Novartis and Ipsen. ST has the following
783 patents filed: Indel mutations as a therapeutic target and predictive biomarker PCTGB2018/051892
784 and PCTGB2018/051893 and Clear Cell Renal Cell Carcinoma Biomarkers P113326GB. N.Y. has
785 received conference support from Celgene. A.R. received a speaker fee from Merck Sharp &
786 Dohme. J.L. has received research funding from Bristol-Myers Squibb, Merck, Novartis, Pfizer,
787 Achilles Therapeutics, Roche, Nektar Therapeutics, Covance, Immunocore, Pharmacyclics, and Aveo,
788 and served as a consultant to Achilles, AstraZeneca, Boston Biomedical, Bristol-Myers Squibb, Eisai,
789 EUSA Pharma, GlaxoSmithKline, Ipsen, Imugene, Incyte, iOnctura, Kymab, Merck Serono, Nektar,
790 Novartis, Pierre Fabre, Pfizer, Roche Genentech, Secarna, and Vitaccess. I.C. has served as a
791 consultant to Eli-Lilly, Bristol Meyers Squibb, MSD, Bayer, Roche, Merck-Serono, Five Prime
792 Therapeutics, Astra-Zeneca, OncXerna, Pierre Fabre, Boehringer Ingelheim, Incyte, Astella, GSK,
793 Sotio, Eisai and has received research funding from Eli-Lilly & Janssen-Cilag. He has received
794 honorarium from Eli-Lilly, Eisai, Servier. A.O. acknowledges receipt of research funding from Pfizer
795 and Roche; speakers fees from Pfizer, Seagen, Lilly and AstraZeneca; is an advisory board member of
796 Roche, Seagen, and AstraZeneca; has received conference support from Leo Pharmaceuticals,
797 AstraZeneca/Diachi-Sankyo and Lilly. C.S. acknowledges grant support from Pfizer, AstraZeneca,
798 Bristol Myers Squibb, Roche-Ventana, Boehringer-Ingelheim, Archer Dx Inc (collaboration in minimal
799 residual disease sequencing technologies) and Ono Pharmaceutical, is an AstraZeneca Advisory
800 Board member and Chief Investigator for the MeRmaiD1 clinical trial, has consulted for Amgen,
801 Pfizer, Novartis, GlaxoSmithKline, MSD, Bristol Myers Squibb, Celgene, AstraZeneca, Illumina,
802 Genentech, Roche-Ventana, GRAIL, Medicxi, Metabomed, Bicycle Therapeutics, and the Sarah
803 Cannon Research Institute, has stock options in Apogen Biotechnologies, Epic Bioscience, GRAIL, and
804 has stock options and is co-founder of Achilles Therapeutics. Patents: C.S. holds European patents
805 relating to assay technology to detect tumour recurrence (PCT/GB2017/053289); to targeting
806 neoantigens (PCT/EP2016/059401), identifying patient response to immune checkpoint blockade
807 (PCT/EP2016/071471), determining HLA LOH (PCT/GB2018/052004), predicting survival rates of
808 patients with cancer (PCT/GB2020/050221), identifying patients who respond to cancer treatment
809 (PCT/GB2018/051912), a US patent relating to detecting tumour mutations (PCT/US2017/28013)
810 and both a European and US patent related to identifying insertion/deletion mutation targets
811 (PCT/GB2018/051892). L.P. has received research funding from Pierre Fabre, and honoraria from

812 Pfizer, Ipsen, Bristol-Myers Squibb, and EUSA Pharma. S.B. has received institutional research
813 funding from Astrazeneca, Tesaro, GSK; speakers fees from Amgen, Pfizer, Astrazeneca, Tesaro, GSK,
814 Clovis, Takeda, Immunogen, Mersana and has an advisor role for Amgen, Astrazeneca, Epsilogen,
815 Genmab, Immunogen, Mersana, MSD, Merck Serono, Oncxerna, Pfizer, Roche. A.R. has received
816 speaker's fee from Merck Sharp & Dohme. Remaining authors have no conflicts of interest to
817 declare.

818

819

820

821 **Tables**822 **Table 1:** CAPTURE cohort overview

	Cohort	SARS-CoV-2 infection	No SARS-CoV2 Infection
Cohort Characteristics	n= 357	n= 118	n= 239
Age, years (median, range)	59 (18-87)	60 (18-87)	60 (26- 82)
Male, n (%)	192 (54)	64 (54)	128 (54)
Cancer diagnosis, n (%)			
Skin	79 (22)	10 (8)	69 (29)
Gastrointestinal	71 (20)	30 (25)	39 (16)
Urology	62 (17)	15 (12)	48 (20)
Lung	41 (11)	8 (7)	33 (14)
Haematological	39 (11)	21 (17)	17 (7)
Breast	31 (9)	16 (13)	16 (7)
Gynaecological	22 (6)	9 (7)	13 (5)
Sarcoma	12 (3)	4 (3)	8 (3)
Head & Neck	6 (2)	5 (4)	1 (0)
Other	4 (1)	4 (3)	0 (0)
Cancer stage, n (%)			
Stage I-II	20 (6)	7 (6)	13 (5)
Stage III	72 (20)	22 (18)	50 (22)
Stage IV	229 (64)	70 (58)	159 (67)
Haematological	39 (11)	21 (17)	17 (7)
Days of Follow up, median (IQR)	154 (63-273)	110 (58-274)	164 (63-274)

823

824 **Table 2.** Oncological and medical history of SARS-CoV-2 positive patients

N=118	
Past medical history	
HTN	31 (27)
PVD/IHD/CVD	9 (8)
Diabetes Mellitus	14 (11)
Obesity, BMI>30, n (%)	25 (21)
Inflammatory/Autoimmune	7 (6)
Smoking status	
Current smoker	36 (31)
Ex-smoker	51 (43)
Never smoked	12 (10)
Unknown	19 (16)
Oncological history	
Solid tumours, n=97	
Disease status (in respect to last treatment)	
SACT, palliative, n=74	
CR/PR	27 (28)
SD	24 (24)
PD	23 (24)
SACT, neoadjuvant or radical CRT	8 (8)
Surgery ± adjuvant SACT	15 (15)
Treatment within 12 weeks	
Systemic therapy	
Chemotherapy	43 (44)
Small molecule inhibitor	15 (15)
Anti-PD(L)1 ± anti-CTLA4	14 (14)
Endocrine therapy	7 (6)
No treatment	5 (4)

Local therapy

Surgery	15 (13)
Radiotherapy	11 (10)

Haematological malignancies, n=21

Diagnosis

Acute leukaemia	11 (52)
Lymphoma	6 (29)
Myeloma	4 (19)

Disease status

MRD/CR	5 (24)
Partial remission	7 (33)
SD	3 (14)
PD/relapse/untreated acute presentation	7 (33)

Treatment within 12 weeks

Chemotherapy	17 (81)
Targeted therapy	10 (48)
Anti-CD20 therapy	6 (29)
CAR-T	1 (5)

Haematologic stem cell transplant

Auto/Allograft pre-COVID-19	6 (29)
Auto/Allograft post-COVID-19	2 (9)

825

826 AS, active surveillance; BMI, body mass index; CAR-T, Chimeric antigen receptor T cell; CD-20, B-
827 lymphocyte antigen; CR, complete response; CRT, chemoradiotherapy; CRP, C-reactive protein;
828 CTLA-4, cytotoxic T-lymphocyte associated protein 4; DM, diabetes mellitus; GVHD, graft versus
829 host disease; Hb, haemoglobin; HTN, hypertension; IHD, ischaemic heart disease; IQR, interquartile
830 range; mAb, monoclonal antibody; MRD, minimal residual disease; NED, no evidence of disease; N0,
831 neutrophil; PCR, polymerase chain reaction; PD progressive disease; PD(L)-1, program death (ligand)
832 -1; Plt, platelet; PVD, peripheral vascular disease; SACT, systemic anti-cancer therapy; SD, stable
833 disease; WBC, white cell blood count; WHO, world health organization

834

835

836

837

838 **Table 3:** Clinical characteristics of COVID-19 illness

COVID-19 characteristics	n (%)
Viral shedding status	
PCR positive, n (%)	95 (81)
Duration of PCR positivity, days median (range)	12 (6-80)
WHO Severity Score	
1, Asymptomatic	24 (20)
2-3, Mild	52 (44)
4-5, Moderate	36 (31)
>5, Severe	6 (5)
Admission to hospital	
Not hospitalised	54 (49)
Admitted with COVID-19- like illness	33 (29)
COVID-19 illness during hospitalisation	30 (25)
Duration of admission, days; median (range)	9 (1 – 120)
Complications of COVID-19	
Required supplemental oxygen	27 (23)
Pneumonia	29 (25)
Venous/arterial thromboembolism	9 (8)
Admission to ITU	7 (6)
Need for mechanical ventilation/NIV	4 (3)
COVID-19 directed therapy	
Corticosteroids	13 (11)
Anti-IL6 mAB	3 (3)
Laboratory Investigations, median (IQR)	
Haematology	
Hb, g/DL	110 (93 – 128)

WBC, x10 ⁶ /L	5.7 (3.4 – 8.0)
NO, x10 ⁶ /L	3.8 (2.1– 5.5)
Plt, x10 ⁶ /L	213 (130 – 299)
Biochemistry	
Creatinine, umol/L	60 (53 – 71)
CRP, mg/L	59 (23 – 134)
Clinical outcomes and impact	
Survival	
Deceased, n (%)	13 (10)
Death within 30 days of PCR positivity	4 (3)
Primary cause death:	
Progressive Cancer	11 (9)
Complications of COVID-19	2 (2)

839

840

CRP, C-reactive protein; Hb, haemoglobin; IL-6, interleukin-6; IQR, interquartile range; mAb, monoclonal antibody; NIV,

841

non-invasive ventilation; NO, neutrophil; PCR, polymerase chain reaction; Plt, platelet; WBC, white cell blood count; WHO,

842

World Health Organization;

843

844

845

846

847

848

849

850

851 **Figure legends**

852 **Figure 1: SARS-CoV-2 infection status, viral shedding, and COVID-19 symptoms of recruited**
853 **patients.**

854 **a)** Patients with cancer irrespective of cancer type, stage, or treatment were recruited. Follow-up
855 schedules for patients with cancer were bespoke to their COVID-19 status and account for their
856 clinical schedules (inpatients: every 2 – 14 days; outpatients: every clinical visit maximum every 3-6
857 weeks in year one and every six months in year two, and at the start of every or every-second cycle
858 of treatment). Clinical data, oronasopharyngeal swabs and blood were collected at each study visit.
859 Viral antigen testing (RT-PCR on swabs), antibody (ELISA, flow cytometric assay), T cell response and
860 IFN- γ activation assays were performed. **b)** Distribution of SARS-CoV-2 infection, and S1-reactive Ab
861 status and COVID-19 severity in patients with cancer. 357 patients with cancer were recruited
862 between May 4, 2020 and March 31st 2021. SARS-CoV-2 infection status by RT-PCR and S1-reactive
863 Ab were analysed at recruitment and in serial samples. RT-PCR results prior to recruitment were
864 extracted from electronic patient records. COVID-19 case definition includes all patients with either
865 RT-PCR confirmed SARS-CoV-2 infection or S1-reactive Ab. **c)** Viral shedding in 43 patients with serial
866 positive swabs. Solid bars indicate time to the last positive test, dotted lines denote the time from
867 the last positive test to the first negative test. **d)** Distribution of symptoms in 118 COVID-19 patients.
868 Bar graph denotes the number of patients. Each row in the lower graph denotes one patient. ONP,
869 Oronasopharyngeal; ELISA, enzyme-linked immunoassay; PBMCs, peripheral blood mononuclear
870 cells; WGS - whole genome sequencing, RTx, radiotherapy, HSCT, human stem cell transplant.

871

872 **Figure 2: S1-reactive and antibody response in patients with cancer**

873 **a)** S1-reactive AbT by COVID-19 severity (n=112 patients). Significance was tested by Kruskal-Wallis
874 test, $p = 0.074$. **b)** S1-reactive AbT by cancer type (Solid patients: n= 92, Haematological patients:
875 n=20). Significance was tested by two-sided Wilcoxon Wilcoxon-Mann-Whitney U test, $p = 0.011$. **c)**
876 NAbT by COVID-19 severity (n=112 patients). Significance was tested by Kruskal-Wallis test, $p =$
877 0.0027 . **d)** NAbT by cancer type (Solid patient: n= 92, Haematological patients: n=20). Significance
878 was tested by two-sided Wilcoxon-Mann-Whitney U test, $p = 0.052$. Boxes indicate 25 and 75
879 percentiles, line indicates median, and whiskers indicate 1.5 times the IQR. Dots represent individual
880 samples. Dotted lines and grey boxes denote the limit of detection. **e)** Multivariate binary logistic
881 regression evaluating association with lack of NAb in patients with cancer (n=112). Wald z-statistic
882 was used two calculate two-sided p-values. *, $p = 0.038$. **f)** Multivariate binary logistic regression
883 evaluating the association of lack of NAb in patients with solid cancer (n = 92). **g)** Multivariate binary

884 logistic regression evaluating the association of lack of NAb in patients with solid cancer (n = 92). Dot
885 denotes odds ratio (blue, positive odds ratio; red, negative odds ratio); whiskers indicate 1.5 times
886 the IQR. **h)** NAbT against WT, Alpha, Beta, and Delta VOCs in patients (n=112) infected with WT
887 SARS-CoV-2 or Alpha VOC. Violin plots denote density of data points. PointRange denotes median
888 and 25 and 75 percentiles. Dots represent individual samples. Significance was tested by Kruskal
889 Wallis test, $p = 3.5e-07$, two-sided Wilcoxon Mann Whitney U-test with Bonferroni correction (post-
890 hoc test) was used for pairwise comparisons. p-values are denoted in the graph. **i)** S1-reactive AbT
891 and **j)** NAbT post onset of disease (n=97 patients). Blue line denotes loess regression line with 95%
892 confidence bands in grey. Black dots denote patients with one sample, coloured dots denote
893 patients with serial samples (n=51 patients). Samples from individual patients are connected. Dotted
894 lines and grey areas at bottom indicate limit of detection. NAb, neutralising antibody, NAbT,
895 neutralising antibody titres, AbT, Antibody titres.

896

897 **Figure 3: T cell response in patients with cancer**

898 **a,b)** Representative plots of $CD4^+CD137^+OX40^+$ ($CD4^+$) and $CD8^+CD137^+CD69^+$ ($CD8^+$) T cells in a
899 patient with confirmed COVID-19 and a cancer patient without COVID-19 after in vitro stimulation
900 with S, M, and N peptide pools, positive control (Staphylococcal enterotoxin B, SEB) or negative
901 control (NC). Frequency of Sars-CoV-2-specific **c)** $CD4^+$ and **d)** $CD8^+$ T cells in solid patients with
902 cancer (n= 83). Frequency of Sars-CoV-2-specific **e)** $CD4^+$ and **f)** $CD8^+$ T cells in haematological
903 patients with cancer (n= 21). Stimulation index was calculated by dividing the percentage of positive
904 cells in the stimulated sample by the percentage of positive cells in the negative control (NC). To
905 obtain the total number of SsT cells the sum of cells activated by S, M, and N was calculated (SMN).
906 Boxes indicate the 25 and 75 percentiles, line indicates the median, and whiskers indicate 1.5 times
907 the IQR. Individual patients are represented as dots. Dots represent individual samples. Dotted lines
908 and grey boxes denote the limit of detection. SsT cells, Sars-CoV-2-specific T cells.

909

910

911 **Figure 4: Comparison of antibody and T cell responses in patients with cancer**

912 **a)** S1-reactive AbT in patients with leukaemia (n=11), myeloma (n=4), and lymphoma (n=6). **b)**
913 Neutralising antibody titres in patients with leukaemia (n=10), myeloma (n=4), and lymphoma (n=6).
914 **c)** $CD4^+$ and $CD8^+$ cells T cells across patients with leukemia (n=10), myeloma (n=4), or lymphoma
915 (n=6). Stimulation index was calculated by dividing the percentage of $CD4^+CD137^+OX40^+$ ($CD4^+$) and
916 $CD8^+CD137^+CD69^+$ ($CD8^+$) T cells in the stimulated sample by the percentage of positive cells in the
917 negative control (NC). Significance was tested by Kruskal-Wallis test, $p < 0.05$ was considered

918 significant. **d)** S1-reactive AbT in patients with haematological malignancy receiving anti-CD20
919 treatment (n=6) vs other SACT (n=15). **e)** NAbT in patients with haematological malignancy receiving
920 anti-CD20 treatment (n=6) vs other SACT (n=15). Significance was tested by two-sided Wilcoxon-
921 Mann-Whitney U test, $p < 0.05$ was considered significant. **f)** Comparison of CD4⁺/CD8⁺ T cells
922 between patients with haematological malignancies on anti-CD20 therapy (n=5, administered within
923 six months) and not on anti-CD20 therapy (n=15). Significance was tested by two-sided Wilcoxon-
924 Mann-Whitney U test, $p < 0.05$ was considered significant. **g)** CD4⁺ and CD8⁺ cells T cells across
925 patients with solid cancer (n=81) by cancer subtype. Boxes indicate the 25 and 75 percentiles, line
926 indicates the median, and whiskers indicate 1.5 times the IQR. Dots represent individual patient
927 samples. Dotted lines and grey boxes denote the limit of detection. Significance was tested by
928 Kruskal-Wallis test, $p < 0.05$ was considered significant. SACT, systemic anti-cancer therapy.

929

930 **Figure 5: Associations between SARS-CoV-2-specific T cells with patient or cancer-specific features**

931 Multivariate binary logistic regression analysis evaluating associations between SARS-CoV-2-specific
932 **a)** CD4⁺ and **b)** CD8⁺ T cells with cancer diagnosis (solid vs haematological malignancies),
933 comorbidities, age, sex, and COVID-19 disease severity in 100 patients. Wald z-statistic was used to
934 calculate two-sided p-values. *, $p = 0.038$. Multivariate binary logistic regression analysis evaluating
935 associations between SARS-CoV-2-specific **c)** CD4⁺ and **d)** CD8⁺ T cells with anti-cancer intervention,
936 age, sex, and COVID-19 disease severity in patients with solid cancer (n=81). Wald z-statistic was
937 used to calculate two-sided p-values. *, $p = 0.045$. Dot denotes odds ratio (blue and red dots
938 indicate positive or negative odds ratio, respectively) ; whiskers indicate 1.5 times the IQR. **e)**
939 Comparison of SARS-CoV-2-specific CD4⁺/CD8⁺ T cells between patients with solid malignancies on
940 CPI (n=13, administered within three months) and not on CPI (n=68). Boxes indicate the 25th and
941 75th percentiles, line indicates the median, and whiskers indicate 1.5 times the IQR. Dots represent
942 individual samples. Significance was tested by two-sided Wilcoxon-Mann-Whitney U test ($p = 0.038$
943 and 0.53).

944

945

946

947

948

949

950

951

952 **References**

- 953 1 Williamson, E. J. et al. Factors associated with COVID-19-related death using OpenSAFELY.
954 Nature 584, 430-436, doi:10.1038/s41586-020-2521-4 (2020).
- 955 2 Saini, K. S. et al. Mortality in patients with cancer and coronavirus disease 2019: A
956 systematic review and pooled analysis of 52 studies. *Eur J Cancer* **139**, 43-50,
957 doi:10.1016/j.ejca.2020.08.011 (2020).
- 958 3 Garcia-Suarez, J. et al. Impact of hematologic malignancy and type of cancer therapy on
959 COVID-19 severity and mortality: lessons from a large population-based registry study. *J Hematol*
960 *Oncol* **13**, 133, doi:10.1186/s13045-020-00970-7 (2020).
- 961 4 Garassino, M. C. et al. COVID-19 in patients with thoracic malignancies (TERAVOLT): first
962 results of an international, registry-based, cohort study. *Lancet Oncol* **21**, 914-922,
963 doi:10.1016/S1470-2045(20)30314-4 (2020).
- 964 5 Lee, L. Y. et al. COVID-19 mortality in patients with cancer on chemotherapy or other
965 anticancer treatments: a prospective cohort study. *Lancet* **395**, 1919-1926, doi:10.1016/S0140-
966 6736(20)31173-9 (2020).
- 967 6 Kuderer, N. M. et al. Clinical impact of COVID-19 on patients with cancer (CCC19): a cohort
968 study. *Lancet* **395**, 1907-1918, doi:10.1016/S0140-6736(20)31187-9 (2020).
- 969 7 Grivas, P. et al. Association of clinical factors and recent anticancer therapy with COVID-19
970 severity among patients with cancer: a report from the COVID-19 and Cancer Consortium. *Ann Oncol*
971 **32**, 787-800, doi:10.1016/j.annonc.2021.02.024 (2021).
- 972 8 Lee, L. Y. W. et al. COVID-19 prevalence and mortality in patients with cancer and the effect
973 of primary tumour subtype and patient demographics: a prospective cohort study. *Lancet Oncol* **21**,
974 1309-1316, doi:10.1016/s1470-2045(20)30442-3 (2020).
- 975 9 Crolley, V. E. et al. COVID-19 in cancer patients on systemic anti-cancer therapies: outcomes
976 from the CAPITOL (COVID-19 Cancer PatienT Outcomes in North London) cohort study. *Ther Adv*
977 *Med Oncol* **12**, 1758835920971147, doi:10.1177/1758835920971147 (2020).
- 978 10 Robilotti, E. V. et al. Determinants of COVID-19 disease severity in patients with cancer. *Nat*
979 *Med*, doi:10.1038/s41591-020-0979-0 (2020).
- 980 11 Bange, E. M. et al. CD8(+) T cells contribute to survival in patients with COVID-19 and
981 hematologic cancer. *Nat Med* **27**, 1280-1289, doi:10.1038/s41591-021-01386-7 (2021).
- 982 12 Abdul-Jawad, S. et al. Acute Immune Signatures and Their Legacies in Severe Acute
983 Respiratory Syndrome Coronavirus-2 Infected Cancer Patients. *Cancer Cell* **39**, 257-275.e256,
984 doi:10.1016/j.ccell.2021.01.001 (2021).

985 13 Thakkar, A. *et al.* Patterns of seroconversion for SARS-CoV-2 IgG in patients with malignant
986 disease and association with anticancer therapy. *Nature Cancer* **2**, 392-399, doi:10.1038/s43018-
987 021-00191-y (2021).

988 14 Au, L. *et al.* Cancer, COVID-19, and Antiviral Immunity: The CAPTURE Study. *Cell* **183**, 4-10,
989 doi:10.1016/j.cell.2020.09.005 (2020).

990 15 A minimal common outcome measure set for COVID-19 clinical research. *Lancet Infect Dis*
991 **20**, e192-e197, doi:10.1016/s1473-3099(20)30483-7 (2020).

992 16 Kuderer, N. M. *et al.* Clinical impact of COVID-19 on patients with cancer (CCC19): a cohort
993 study. *Lancet* **395**, 1907-1918, doi:10.1016/s0140-6736(20)31187-9 (2020).

994 17 Lowe, K. E., Zein, J., Hatipoglu, U. & Attaway, A. Association of Smoking and Cumulative
995 Pack-Year Exposure With COVID-19 Outcomes in the Cleveland Clinic COVID-19 Registry. *JAMA*
996 *Intern Med* **181**, 709-711, doi:10.1001/jamainternmed.2020.8360 (2021).

997 18 Sterlin, D. *et al.* IgA dominates the early neutralizing antibody response to SARS-CoV-2. *Sci.*
998 *Transl. Med.* **13**, eabd2223, doi:10.1126/scitranslmed.abd2223 (2021).

999 19 Grifoni, A. *et al.* Targets of T Cell Responses to SARS-CoV-2 Coronavirus in Humans with
1000 COVID-19 Disease and Unexposed Individuals. *Cell*, doi:10.1016/j.cell.2020.05.015.

1001 20 Dan, J. M. *et al.* Immunological memory to SARS-CoV-2 assessed for up to 8 months after
1002 infection. *Science* **371**, eabf4063, doi:10.1126/science.abf4063 (2021).

1003 21 Moderbacher, C. R. *et al.* Antigen-specific adaptive immunity to SARS-CoV-2 in acute COVID-
1004 19 and associations with age and disease severity. *Cell*, doi:10.1016/j.cell.2020.09.038 (2020).

1005 22 Weiskopf, D. *et al.* Phenotype and kinetics of SARS-CoV-2-specific T cells in COVID-19
1006 patients with acute respiratory distress syndrome. *Science immunology* **5**, eabd2071,
1007 doi:10.1126/sciimmunol.abd2071 (2020).

1008 23 Crotty, S. T Follicular Helper Cell Biology: A Decade of Discovery and Diseases. *Immunity* **50**,
1009 1132-1148, doi:<https://doi.org/10.1016/j.immuni.2019.04.011> (2019).

1010 24 Mateus, J. *et al.* Selective and cross-reactive SARS-CoV-2 T cell epitopes in unexposed
1011 humans. *Science*, eabd3871, doi:10.1126/science.abd3871 (2020).

1012 25 Marra, A. *et al.* Seroconversion in patients with cancer and oncology health care workers
1013 infected by SARS-CoV-2. *Ann Oncol* **32**, 113-119, doi:10.1016/j.annonc.2020.10.473 (2021).

1014 26 Earle, K. A. *et al.* Evidence for antibody as a protective correlate for COVID-19 vaccines.
1015 *Vaccine* **39**, 4423-4428, doi:<https://doi.org/10.1016/j.vaccine.2021.05.063> (2021).

1016 27 Khoury, D. S. *et al.* Neutralizing antibody levels are highly predictive of immune protection
1017 from symptomatic SARS-CoV-2 infection. *Nature Medicine* **27**, 1205-1211, doi:10.1038/s41591-021-
1018 01377-8 (2021).

1019 28 Seow, J. *et al.* Longitudinal observation and decline of neutralizing antibody responses in the
1020 three months following SARS-CoV-2 infection in humans. *Nature Microbiology* **5**, 1598-1607,
1021 doi:10.1038/s41564-020-00813-8 (2020).

1022 29 Gaebler, C. *et al.* Evolution of antibody immunity to SARS-CoV-2. *Nature* **591**, 639-644,
1023 doi:10.1038/s41586-021-03207-w (2021).

1024 30 Wang, Z. *et al.* Naturally enhanced neutralizing breadth against SARS-CoV-2 one year after
1025 infection. *Nature* **595**, 426-431, doi:10.1038/s41586-021-03696-9 (2021).

1026 31 Achiron, A. *et al.* SARS-CoV-2 antibody dynamics and B-cell memory response over time in
1027 COVID-19 convalescent subjects. *Clin Microbiol Infect*, doi:10.1016/j.cmi.2021.05.008 (2021).

1028 32 Vacharathit, V. *et al.* SARS-CoV-2 variants of concern exhibit reduced sensitivity to live-virus
1029 neutralization in sera from CoronaVac vaccinees and naturally infected COVID-19 patients. medRxiv,
1030 2021.2007.2010.21260232, doi:10.1101/2021.07.10.21260232 (2021).

1031 33 Juno, J. A. *et al.* Humoral and circulating follicular helper T cell responses in recovered
1032 patients with COVID-19. *Nature Medicine* **26**, 1428-1434, doi:10.1038/s41591-020-0995-0 (2020).

1033 34 Murugesan, K. *et al.* Interferon-gamma release assay for accurate detection of SARS-CoV-2 T
1034 cell response. *Clinical Infectious Diseases*, doi:10.1093/cid/ciaa1537 (2020).

1035 35 Pauken, K. E. *et al.* The PD-1 Pathway Regulates Development and Function of Memory
1036 CD8⁺ T Cells following Respiratory Viral Infection. *Cell Reports* **31**,
1037 doi:10.1016/j.celrep.2020.107827 (2020).

1038 36 Konkel, J. E. *et al.* PD-1 signalling in CD4(+) T cells restrains their clonal expansion to an
1039 immunogenic stimulus, but is not critically required for peptide-induced tolerance. *Immunology* **130**,
1040 92-102, doi:10.1111/j.1365-2567.2009.03216.x (2010).

1041 37 Apostolidis, S. A. *et al.* Altered cellular and humoral immune responses following SARS-CoV-
1042 2 mRNA vaccination in patients with multiple sclerosis on anti-CD20 therapy. medRxiv,
1043 2021.2006.2023.21259389, doi:10.1101/2021.06.23.21259389 (2021).

1044 38 Zhao, J., Zhao, J. & Perlman, S. T cell responses are required for protection from clinical
1045 disease and for virus clearance in severe acute respiratory syndrome coronavirus-infected mice. *J.*
1046 *Virol.* **84**, 9318-9325, doi:10.1128/jvi.01049-10 (2010).

1047 39 Tan, A. T. *et al.* Early induction of functional SARS-CoV-2-specific T cells associates with rapid
1048 viral clearance and mild disease in COVID-19 patients. *Cell Rep.* **34**, 108728,
1049 doi:https://doi.org/10.1016/j.celrep.2021.108728 (2021).

1050 40 Muñoz-Fontela, C. *et al.* Animal models for COVID-19. *Nature* **586**, 509-515,
1051 doi:10.1038/s41586-020-2787-6 (2020).

1052 41 Sahin, U. et al. COVID-19 vaccine BNT162b1 elicits human antibody and T(H)1 T cell
1053 responses. *Nature* 586, 594-599, doi:10.1038/s41586-020-2814-7 (2020).

1054 42 Ewer, K. J. et al. T cell and antibody responses induced by a single dose of ChAdOx1 nCoV-19
1055 (AZD1222) vaccine in a phase 1/2 clinical trial. *Nat. Med.* 27, 270-278, doi:10.1038/s41591-020-
1056 01194-5 (2021).

1057 43 Tarke, A. et al. Impact of SARS-CoV-2 variants on the total CD4(+) and CD8(+) T cell reactivity
1058 in infected or vaccinated individuals. *Cell Rep Med* 2, 100355, doi:10.1016/j.xcrm.2021.100355
1059 (2021).

1060 44 Sekine, T. et al. Robust T Cell Immunity in Convalescent Individuals with Asymptomatic or
1061 Mild COVID-19. *Cell* 183, 158-168.e114, doi:https://doi.org/10.1016/j.cell.2020.08.017 (2020).

1062 45 Le Bert, N. et al. SARS-CoV-2-specific T cell immunity in cases of COVID-19 and SARS, and
1063 uninfected controls. *Nature* 584, 457-462, doi:10.1038/s41586-020-2550-z (2020).

1064 46 Angelis, V. *et al.* Defining the true impact of coronavirus disease 2019 in the at-risk
1065 population of patients with cancer. *Eur J Cancer* **136**, 99-106, doi:10.1016/j.ejca.2020.06.027 (2020).
1066
1067

1068 **Methods-only references**

1069

1070 47 Aitken, J. et al. Scalable and robust SARS-CoV-2 testing in an academic center. Nat.
1071 Biotechnol., doi:10.1038/s41587-020-0588-y (2020).

1072 48 Di Tommaso, P. et al. Nextflow enables reproducible computational workflows. Nat
1073 Biotechnol 35, 316-319, doi:10.1038/nbt.3820 (2017).

1074 49 Baker, D. J. et al. CoronaHiT: high-throughput sequencing of SARS-CoV-2 genomes. Genome
1075 Med. 13, 21, doi:10.1186/s13073-021-00839-5 (2021).

1076 50 Ewels, P. A. et al. The nf-core framework for community-curated bioinformatics pipelines.
1077 Nat Biotechnol 38, 276-278, doi:10.1038/s41587-020-0439-x (2020).

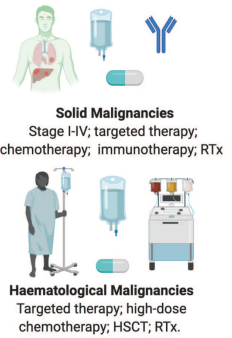
1078 51. Faulkner, N., et al., Reduced antibody cross-reactivity following infection with B.1.1.7 than
1079 with parental SARS-CoV-2 strains. bioRxiv, 2021: p. 2021.03.01.433314.

1080 52. Rihn, S.J., et al., A plasmid DNA-launched SARS-CoV-2 reverse genetics system and
1081 coronavirus toolkit for COVID-19 research. PLoS Biol, 2021. 19(2): p. e3001091.

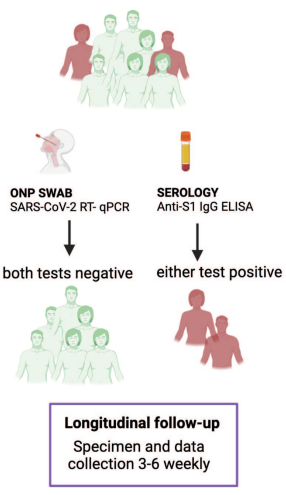
a The CAPTURE Study

PROSPECTIVE RECRUITMENT

- INCLUSION CRITERIA**
- >18 years in age
 - Any confirmed cancer diagnosis
- EXCLUSION CRITERIA**
- Condition that precludes informed consent

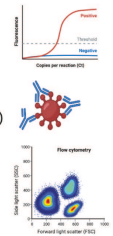


SARS-CoV-2 CASE DEFINITION



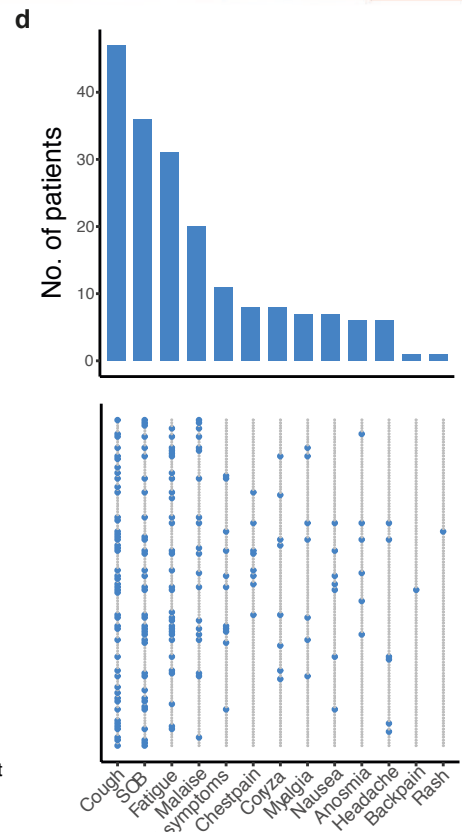
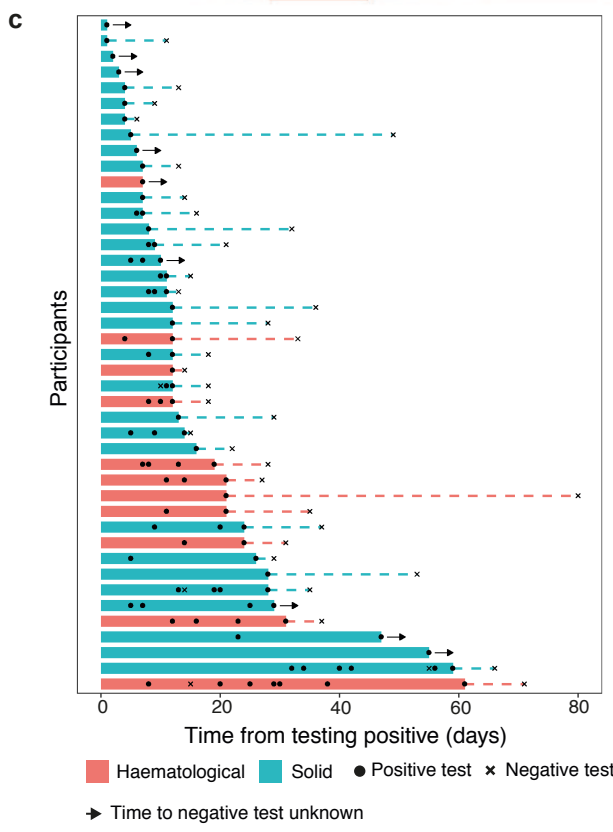
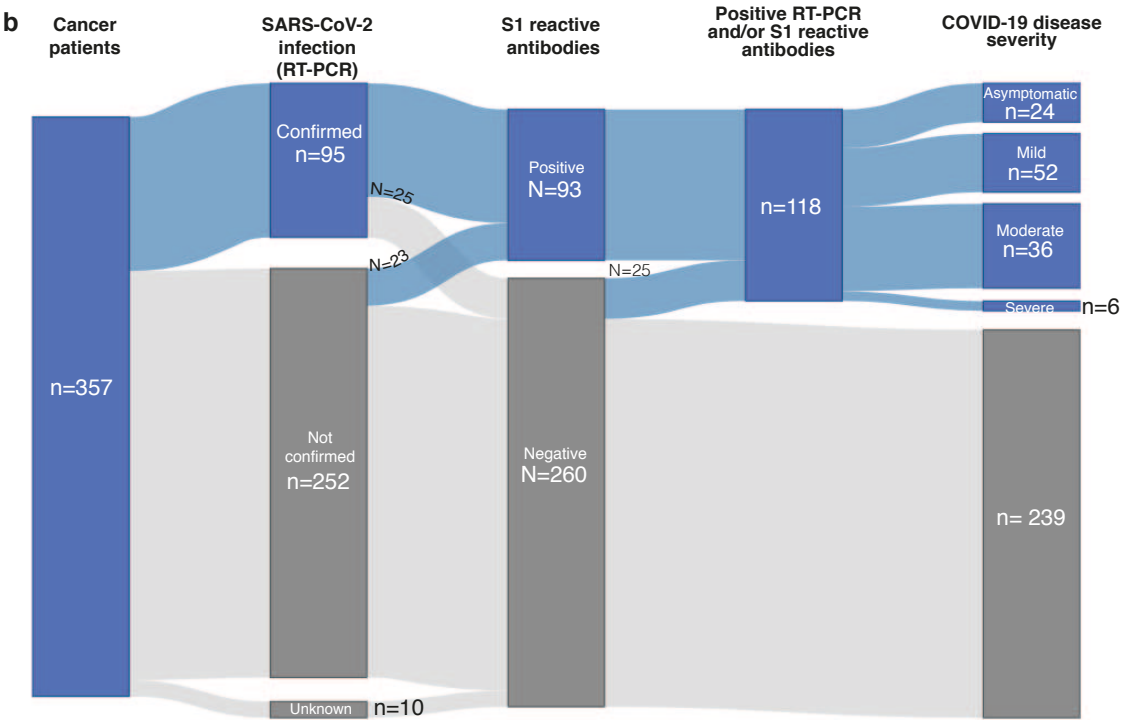
BIOSPECIMENS & LABORATORY ASSAYS

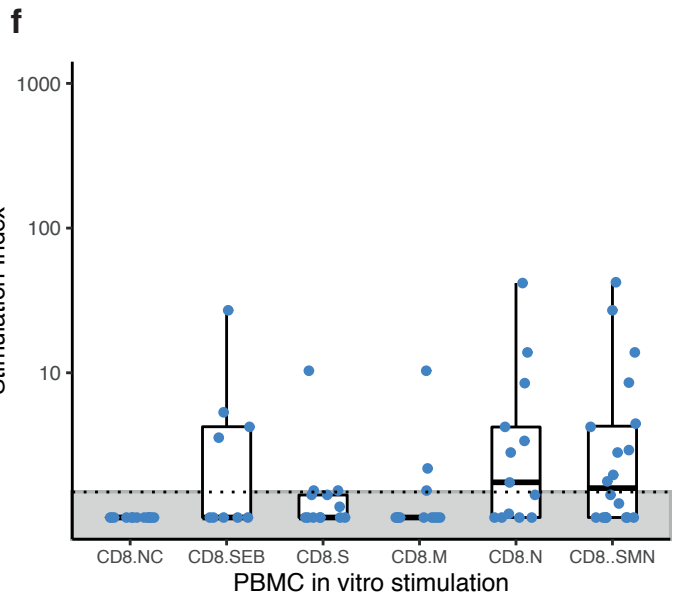
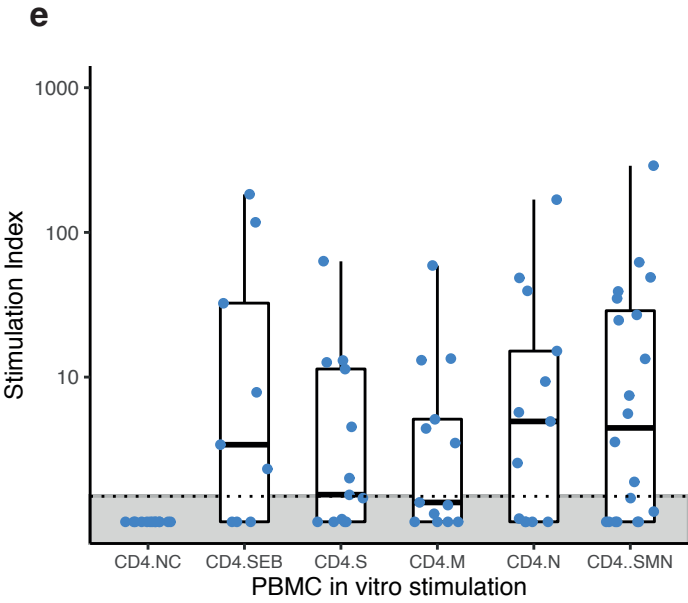
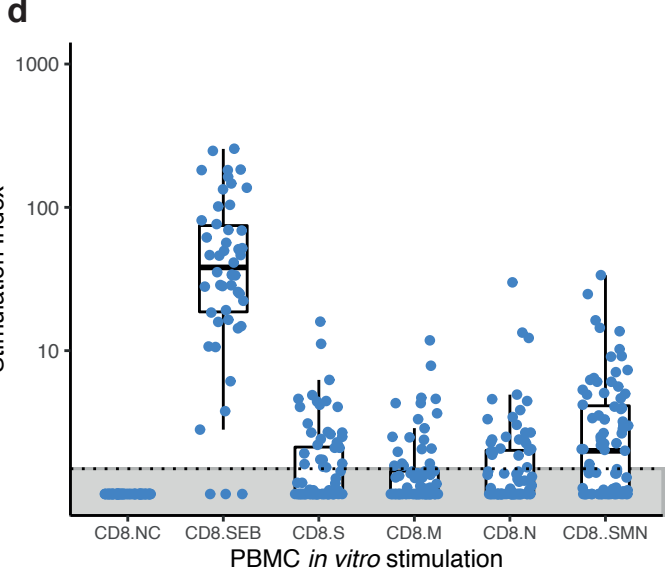
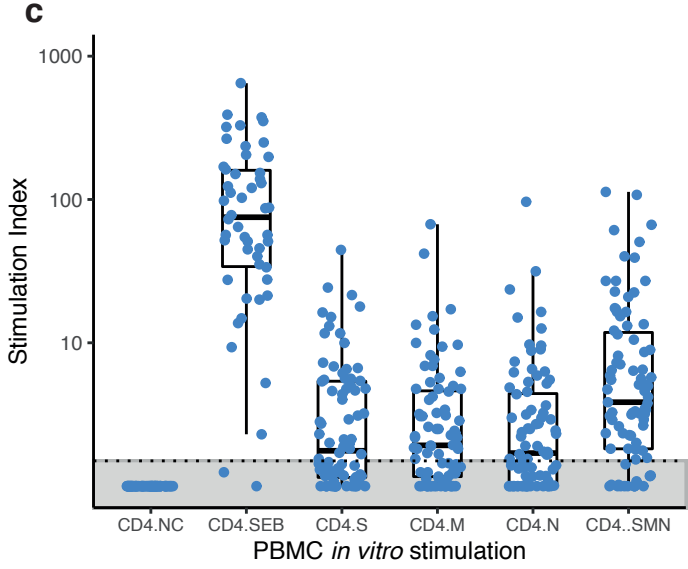
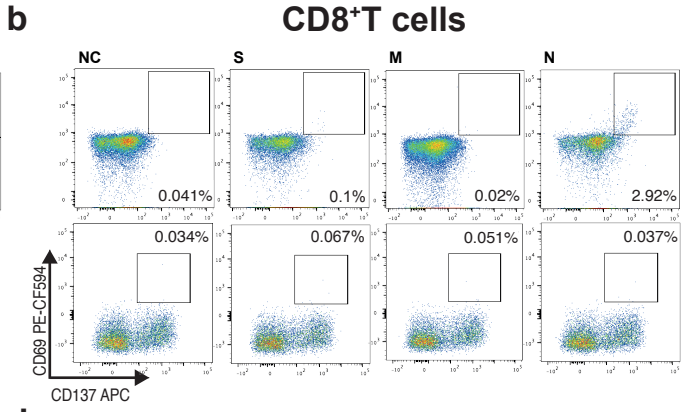
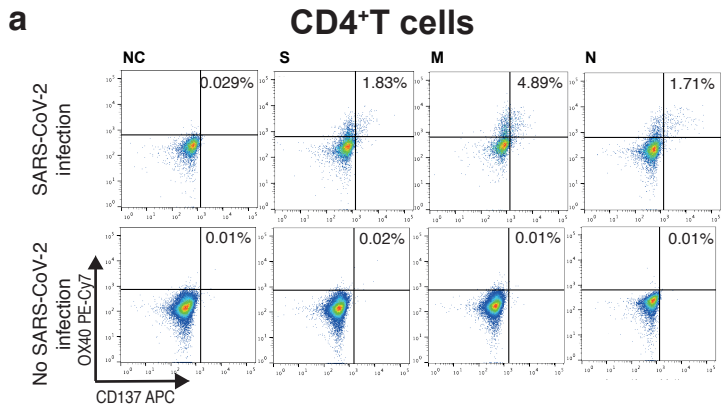
- ONP SWAB**
- SARS-CoV-2 RT- qPCR
 - SARS-CoV-2 WGS*
- SERUM/PLASMA**
- Antibody response (ELISA & Flow)
 - Neutralising Ab response
 - Cytokine and chemokine profiling
- PBMCs**
- T-cell response & IFN-γ activation

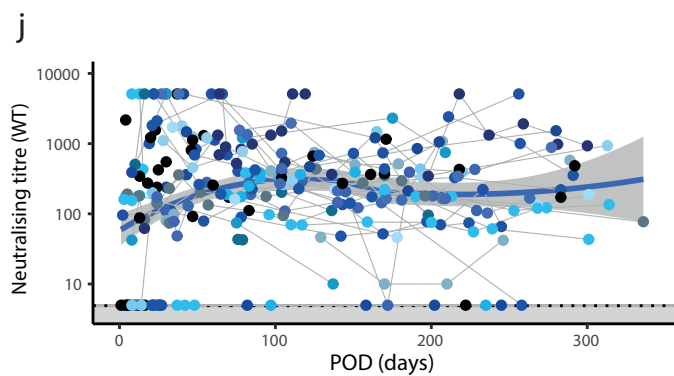
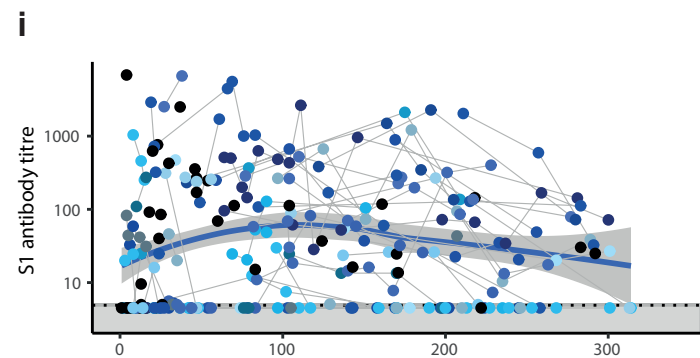
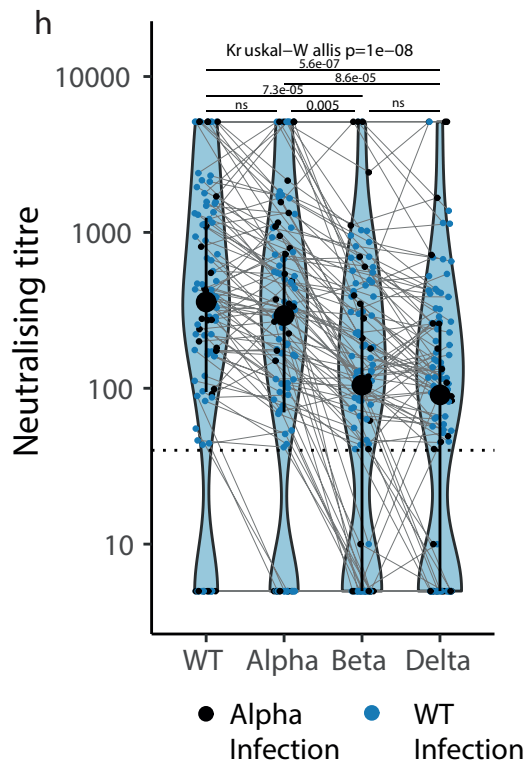
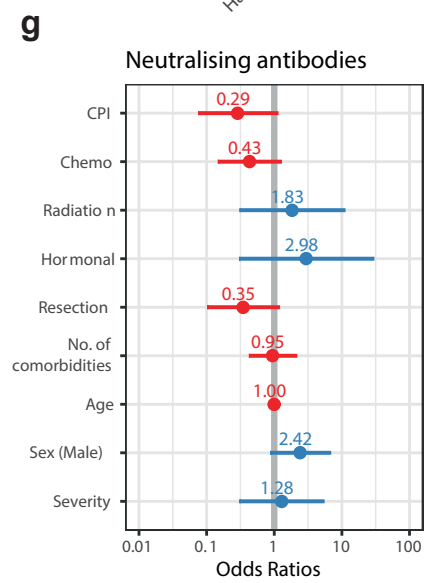
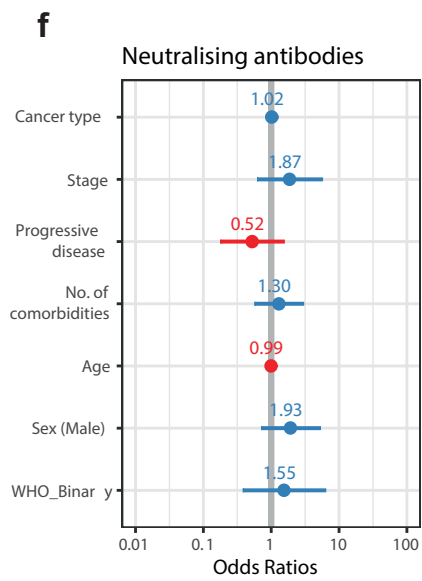
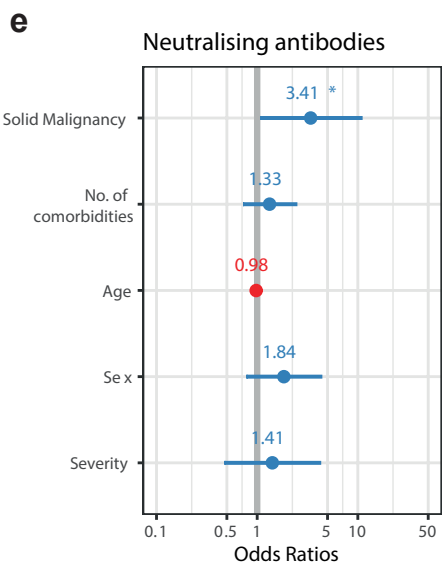
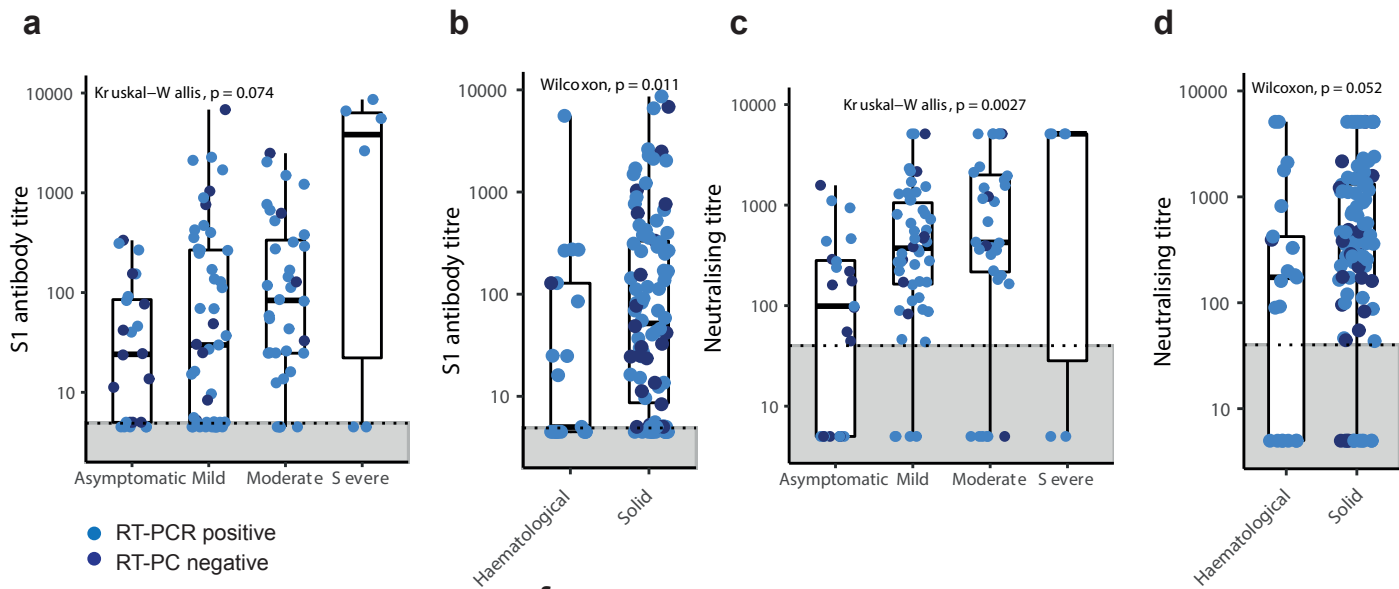


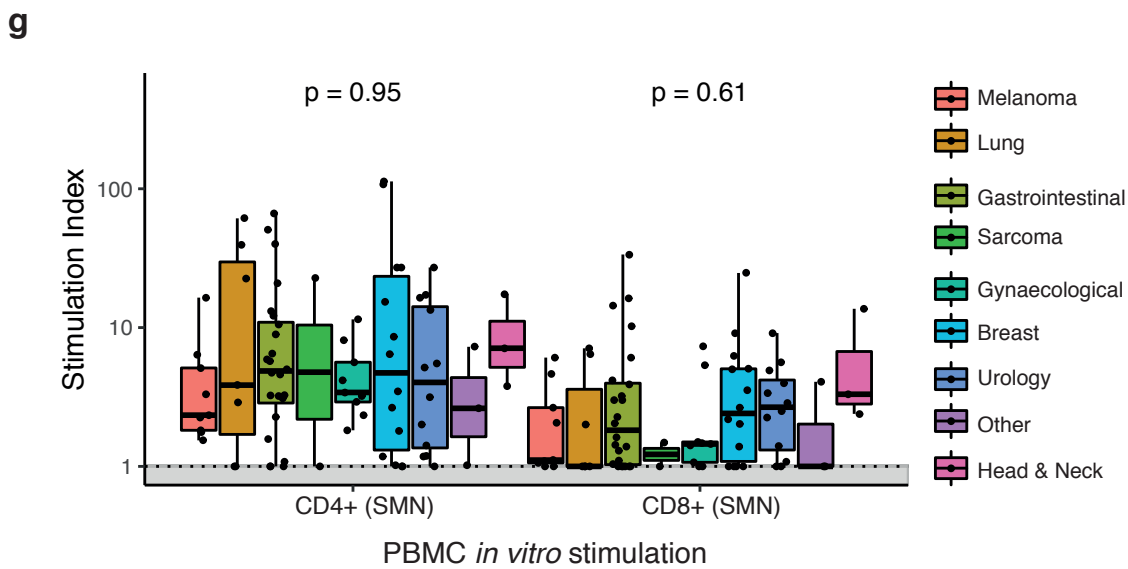
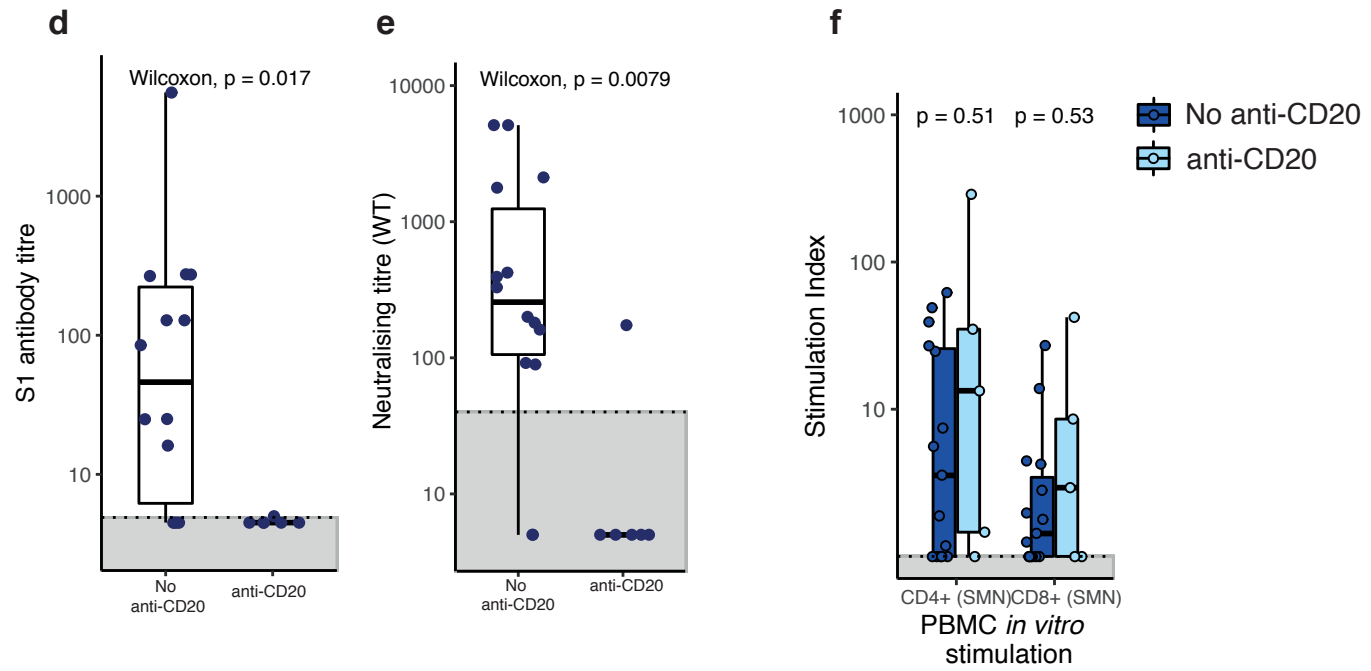
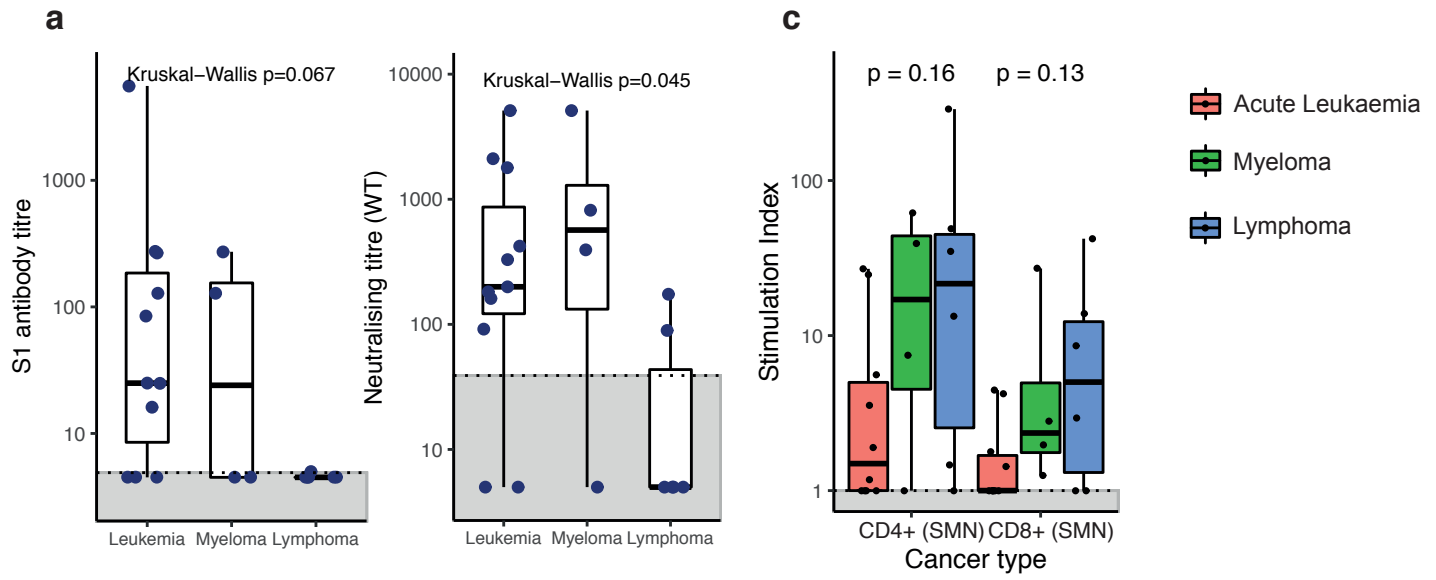
COMPREHENSIVE DATA COLLECTION

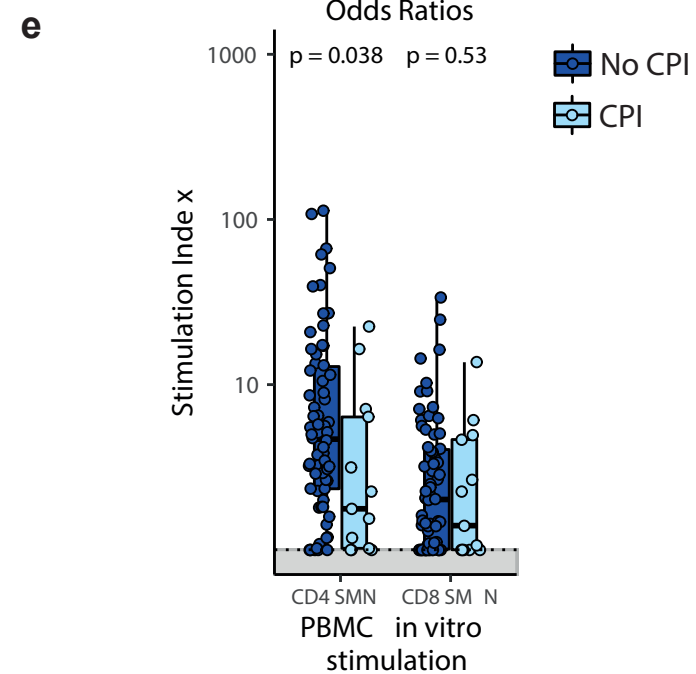
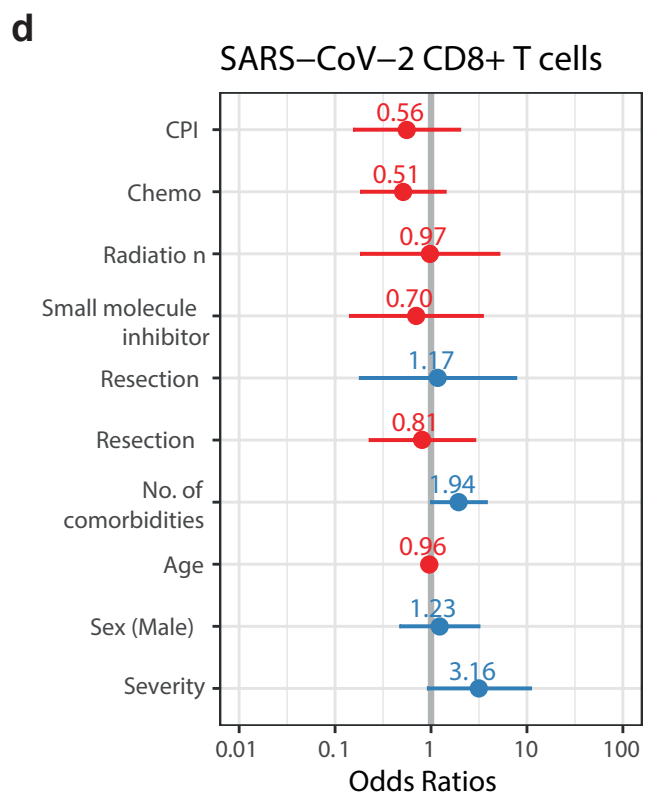
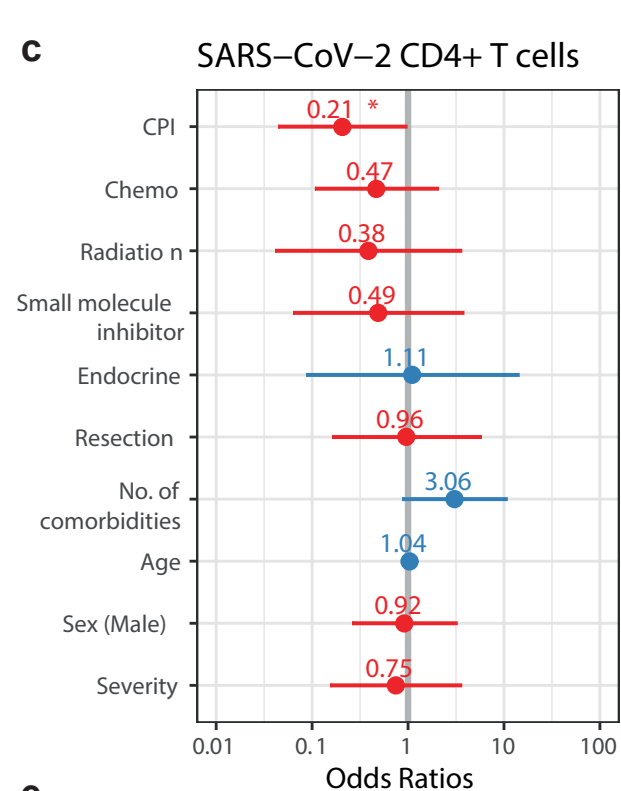
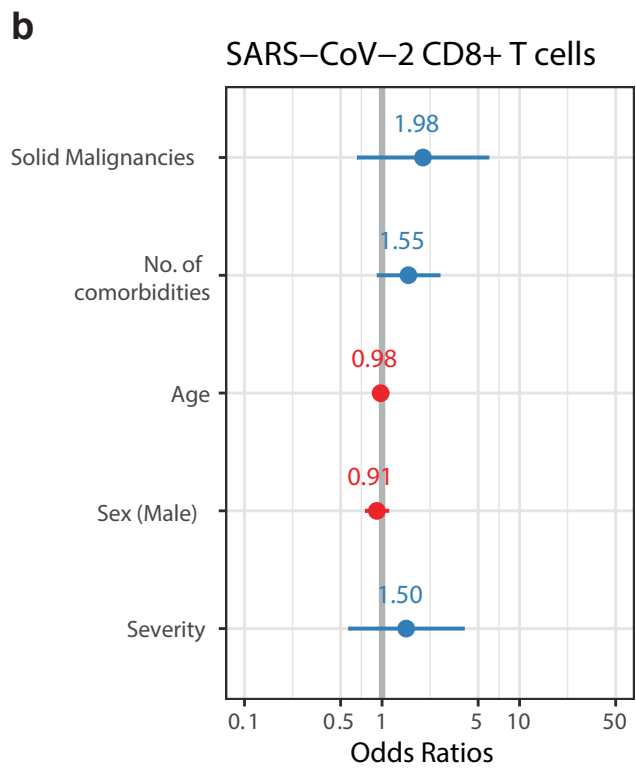
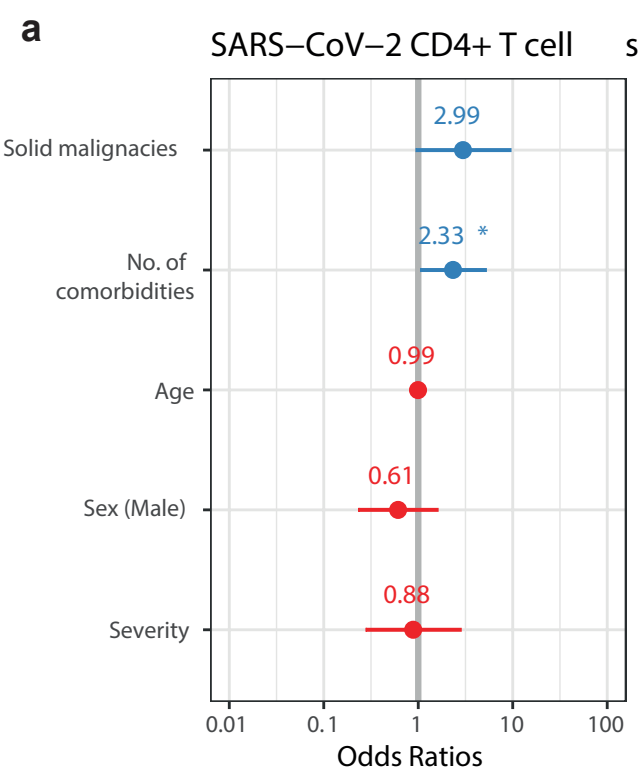
- Electronic Case Report Form (eCRF)**
- Containing 135 data points
 - Demographic and past medical history
 - Oncological treatment history
 - Standard of care diagnostic laboratory and radiology results











Figures

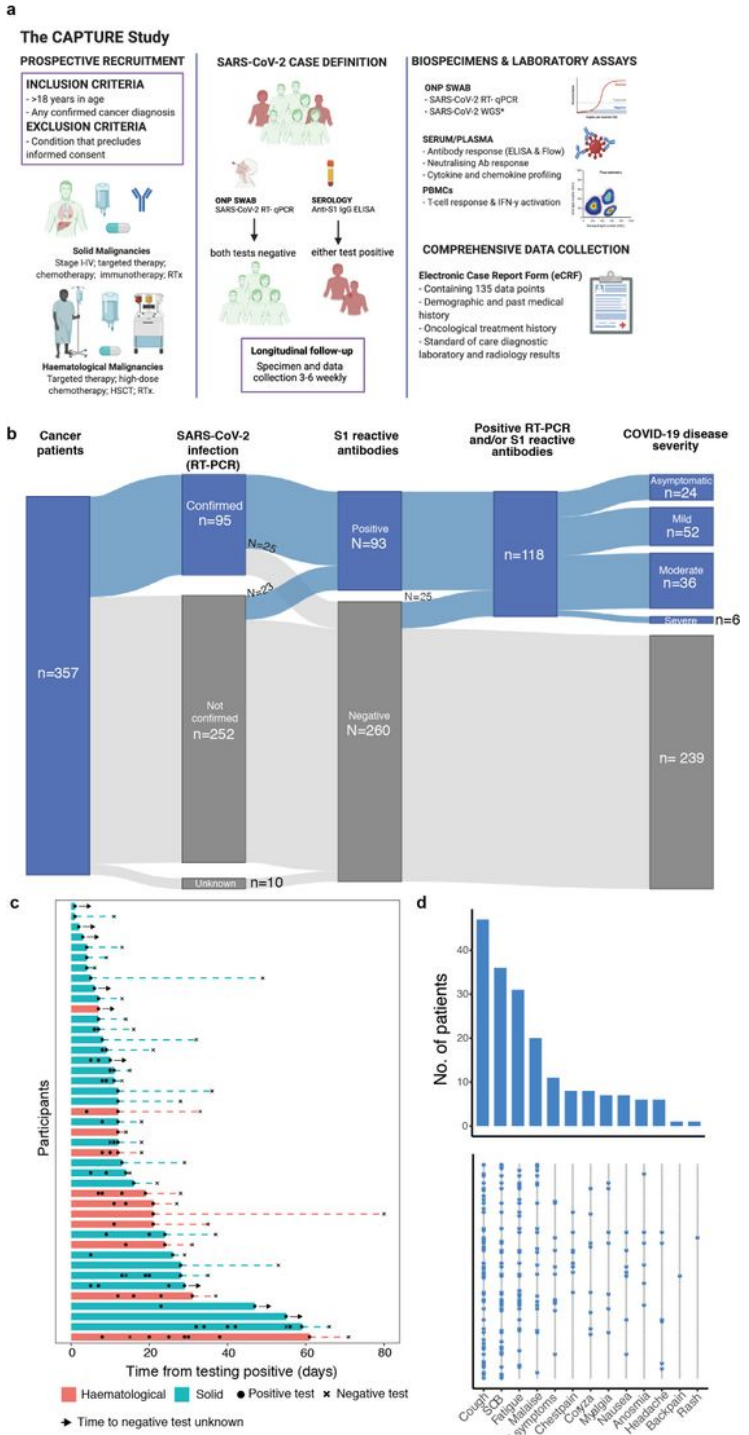


Figure 1

SARS-CoV-2 infection status, viral shedding, and COVID-19 symptoms of recruited patients. a) Patients with cancer irrespective of cancer type, stage, or treatment were recruited. Follow-up schedules for patients with cancer were bespoke to their COVID-19 status and account for their clinical schedules

(inpatients: every 2 – 14 days; outpatients: every clinical visit maximum every 3-6 weeks in year one and every six months in year two, and at the start of every or every-second cycle of treatment). Clinical data, oronasopharyngeal swabs and blood were collected at each study visit. Viral antigen testing (RT-PCR on swabs), antibody (ELISA, flow cytometric assay), T cell response and IFN- γ activation assays were performed. b) Distribution of SARS-CoV-2 infection, and S1-reactive Ab status and COVID-19 severity in patients with cancer. 357 patients with cancer were recruited between May 4, 2020 and March 31st 2021. SARS-CoV-2 infection status by RT-PCR and S1-reactive Ab were analysed at recruitment and in serial samples. RT-PCR results prior to recruitment were extracted from electronic patient records. COVID-19 case definition includes all patients with either RT-PCR confirmed SARS-CoV-2 infection or S1-reactive Ab. c) Viral shedding in 43 patients with serial positive swabs. Solid bars indicate time to the last positive test, dotted lines denote the time from the last positive test to the first negative test. d) Distribution of symptoms in 118 COVID-19 patients. Bar graph denotes the number of patients. Each row in the lower graph denotes one patient. ONP, Oronasopharyngeal; ELISA, enzyme-linked immunoassay; PBMCs, peripheral blood mononuclear cells; WGS - whole genome sequencing, RTx, radiotherapy, HSCT, human stem cell transplant.

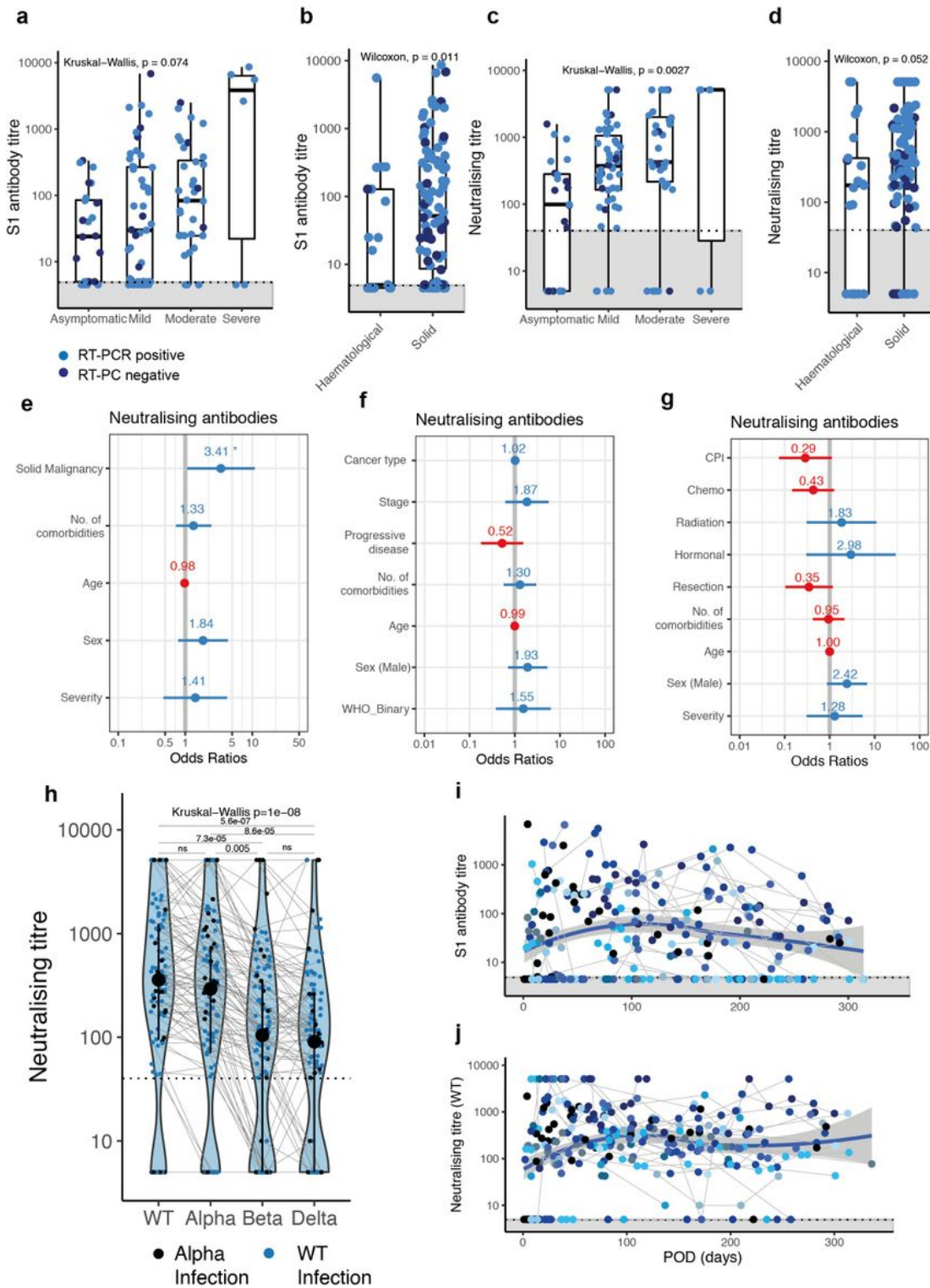


Figure 2

S1-reactive and antibody response in patients with cancer a) S1-reactive AbT by COVID-19 severity (n=112 patients). Significance was tested by Kruskal-Wallis test, $p = 0.074$. b) S1-reactive AbT by cancer type (Solid patients: n= 92, Haematological patients: n=20). Significance was tested by two-sided Wilcoxon Wilcoxon-Mann-Whitney U test, $p = 0.011$. c) NAbT by COVID-19 severity (n=112 patients). Significance was tested by Kruskal-Wallis test, $p = 0.0027$. d) NAbT by cancer type (Solid patient: n= 92,

Haematological patients: n=20). Significance was tested by two-sided Wilcoxon-Mann-Whitney U test, $p = 0.052$. Boxes indicate 25 and 75 percentiles, line indicates median, and whiskers indicate 1.5 times the IQR. Dots represent individual samples. Dotted lines and grey boxes denote the limit of detection. e) Multivariate binary logistic regression evaluating association with lack of NAb in patients with cancer (n=112). Wald z-statistic was used to calculate two-sided p-values. *, $p = 0.038$. f) Multivariate binary logistic regression evaluating the association of lack of NAb in patients with solid cancer (n = 92). g) Multivariate binary logistic regression evaluating the association of lack of NAb in patients with solid cancer (n = 92). Dot denotes odds ratio (blue, positive odds ratio; red, negative odds ratio); whiskers indicate 1.5 times the IQR. h) NAbT against WT, Alpha, Beta, and Delta VOCs in patients (n=112) infected with WT SARS-CoV-2 or Alpha VOC. Violin plots denote density of data points. PointRange denotes median and 25 and 75 percentiles. Dots represent individual samples. Significance was tested by Kruskal Wallis test, $p = 3.5e-07$, two-sided Wilcoxon Mann Whitney U-test with Bonferroni correction (post-hoc test) was used for pairwise comparisons. p-values are denoted in the graph. i) S1-reactive AbT and j) NAbT post onset of disease (n=97 patients). Blue line denotes loess regression line with 95% confidence bands in grey. Black dots denote patients with one sample, coloured dots denote patients with serial samples (n=51 patients). Samples from individual patients are connected. Dotted lines and grey areas at bottom indicate limit of detection. NAb, neutralising antibody, NAbT, neutralising antibody titres, AbT, Antibody titres.

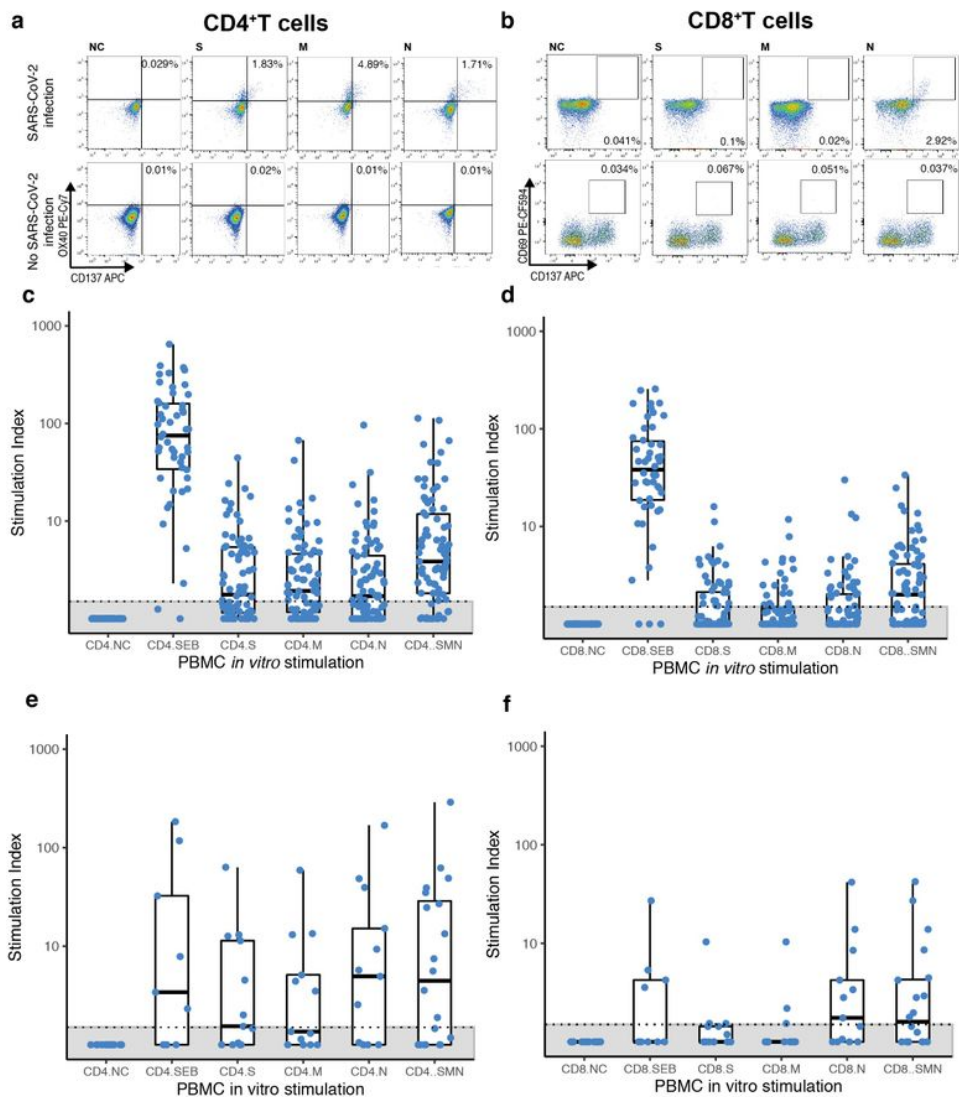


Figure 3

T cell response in patients with cancer a,b) Representative plots of CD4⁺CD137⁺OX40⁺ (CD4⁺) and CD8⁺CD137⁺CD69⁺ (CD8⁺) T cells in a patient with confirmed COVID-19 and a cancer patient without COVID-19 after *in vitro* stimulation with S, M, and N peptide pools, positive control (Staphylococcal enterotoxin B, SEB) or negative control (NC). Frequency of Sars-CoV-2-specific c) CD4⁺ and d) CD8⁺ T cells in solid patients with cancer (n= 83). Frequency of Sars-CoV-2-specific e) CD4⁺ and f) CD8⁺ T cells in haematological patients with cancer (n= 21). Stimulation index was calculated by dividing the

percentage of positive cells in the stimulated sample by the percentage of positive cells in the negative control (NC). To obtain the total number of SsT cells the sum of cells activated by S, M, and N was calculated (SMN). Boxes indicate the 25 and 75 percentiles, line indicates the median, and whiskers indicate 1.5 times the IQR. Individual patients are represented as dots. Dots represent individual samples. Dotted lines and grey boxes denote the limit of detection. SsT cells, Sars-CoV-2-specific T cells.

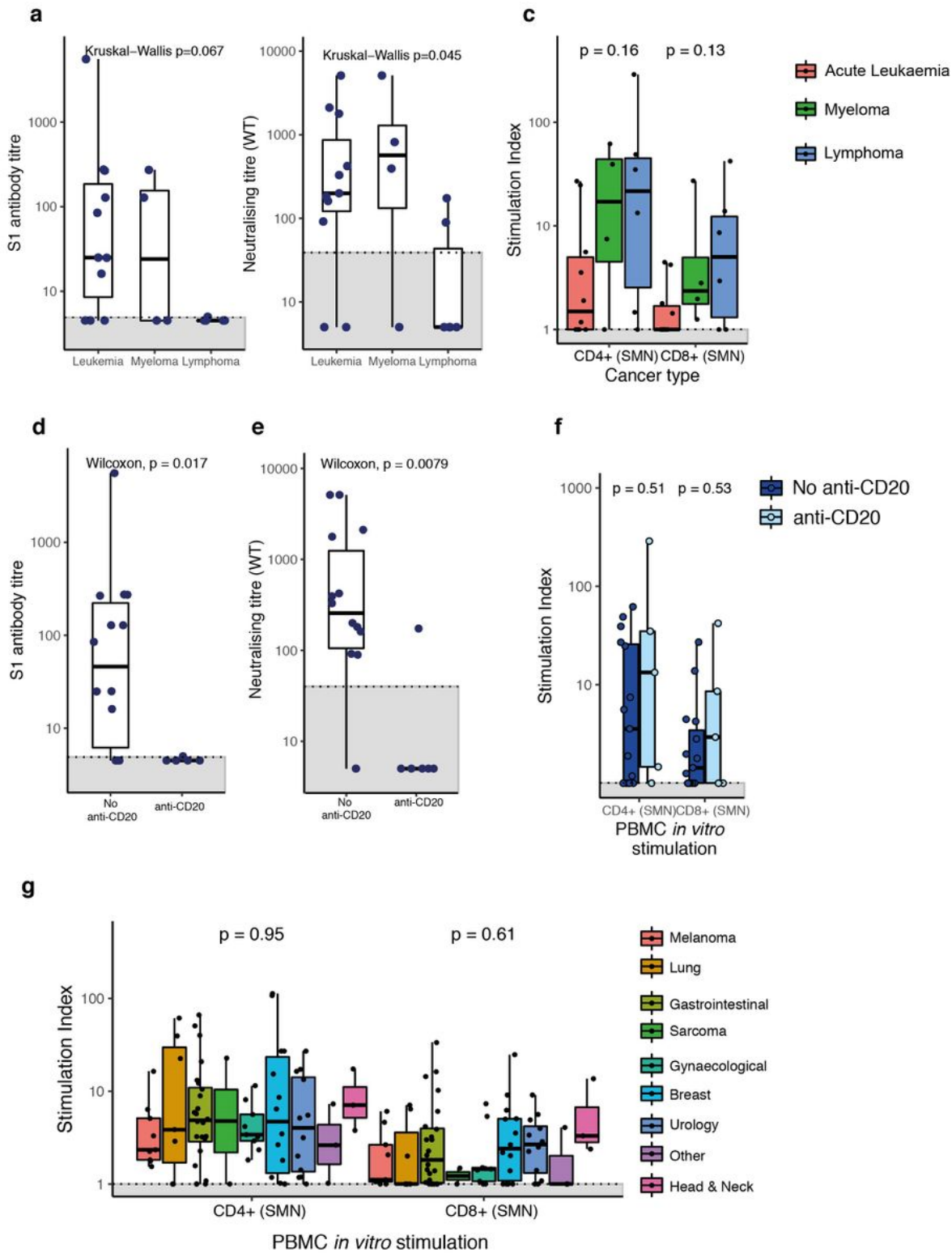


Figure 4

Comparison of antibody and T cell responses in patients with cancer a) S1-reactive AbT in patients with leukaemia (n=11), myeloma (n=4), and lymphoma (n=6). b) Neutralising antibody titres in patients with leukaemia (n=10), myeloma (n=4), and lymphoma (n=6). c) CD4+ and CD8+ cells T cells across patients with leukemia (n=10), myeloma (n=4), or lymphoma (n=6). Stimulation index was calculated by dividing the percentage of CD4+CD137+OX40+ (CD4+) and CD8+CD137+CD69+ (CD8+) T cells in the stimulated sample by the percentage of positive cells in the negative control (NC). Significance was tested by Kruskal-Wallis test, $p < 0.05$ was considered significant. d) S1-reactive AbT in patients with haematological malignancy receiving anti-CD20 treatment (n=6) vs other SACT (n=15). e) NAbT in patients with haematological malignancy receiving anti-CD20 treatment (n=6) vs other SACT (n=15). Significance was tested by two-sided Wilcoxon-Mann-Whitney U test, $p < 0.05$ was considered significant. f) Comparison of CD4+/CD8+ T cells between patients with haematological malignancies on anti-CD20 therapy (n=5, administered within six months) and not on anti-CD20 therapy (n=15). Significance was tested by two-sided Wilcoxon-Mann-Whitney U test, $p < 0.05$ was considered significant. g) CD4+ and CD8+ cells T cells across patients with solid cancer (n=81) by cancer subtype. Boxes indicate the 25 and 75 percentiles, line indicates the median, and whiskers indicate 1.5 times the IQR. Dots represent individual patient samples. Dotted lines and grey boxes denote the limit of detection. Significance was tested by Kruskal-Wallis test, $p < 0.05$ was considered significant. SACT, systemic anti-cancer therapy.

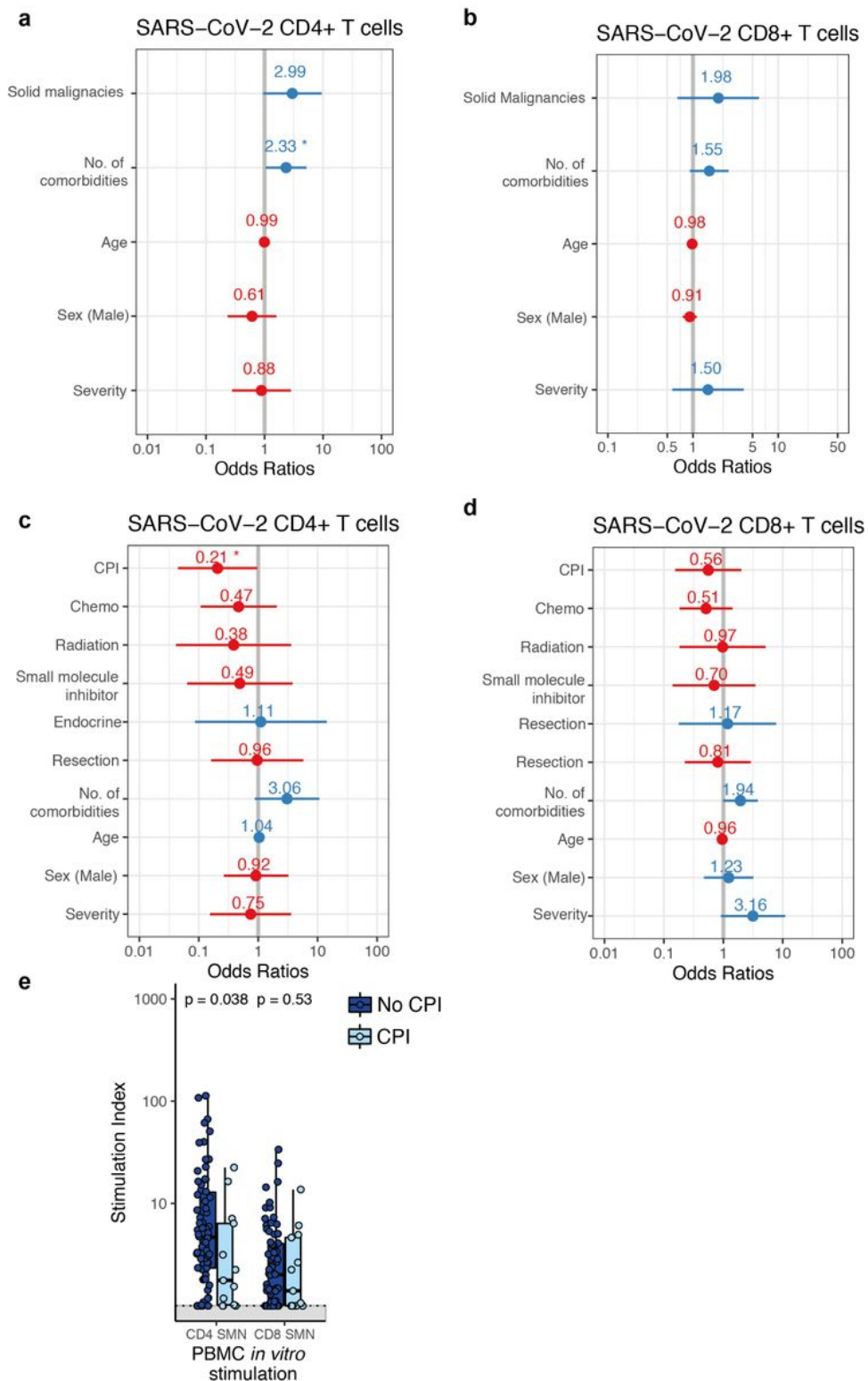


Figure 5

Associations between SARS-CoV-2-specific T cells with patient or cancer-specific features Multivariate binary logistic regression analysis evaluating associations between SARS-CoV-2-specific a) CD4+ and b) CD8+ T cells with cancer diagnosis (solid vs haematological malignancies), comorbidities, age, sex, and COVID-19 disease severity in 100 patients. Wald z-statistic was used to calculate two-sided p-values. *, $p = 0.038$. Multivariate binary logistic regression analysis evaluating associations between SARS-CoV-2-

specific c) CD4+ and d) CD8+ T cells with anti-cancer intervention, age, sex, and COVID-19 disease severity in patients with solid cancer (n=81). Wald z-statistic was used to calculate two-sided p-values. *, $p = 0.045$. Dot denotes odds ratio (blue and red dots indicate positive or negative odds ratio, respectively) ; whiskers indicate 1.5 times the IQR. e) Comparison of SARS-CoV-2-specific CD4+/CD8+ T cells between patients with solid malignancies on CPI (n=13, administered within three months) and not on CPI (n=68). Boxes indicate the 25th and 75th percentiles, line indicates the median, and whiskers indicate 1.5 times the IQR. Dots represent individual samples. Significance was tested by two-sided Wilcoxon-Mann-Whitney U test ($p = 0.038$ and 0.53).

Supplementary Files

This is a list of supplementary files associated with this preprint. Click to download.

- [ExtendedFigure1infection.png](#)
- [ExtendedFigure2infection.png](#)
- [ExtendedFigure3Infection.png](#)
- [ExtendedFigure4Infection.png](#)
- [ExtendedFigure5Infection.png](#)
- [ExtendedFigure6infection.png](#)
- [SupplementaryTable1infection.pdf](#)
- [SupplementaryTable2infection.pdf](#)
- [SupplementaryTable3Infection.pdf](#)